

# THE ADAPTIVE PATCHED PARTICLE FILTER AND ITS IMPLEMENTATION

BY WONJUNG LEE\* AND TERRY LYONS\*

*University of Oxford\**

There are numerous contexts where one wishes to describe the state of a randomly evolving system. Effective solutions combine models that quantify the underlying uncertainty with available observational data to form relatively optimal estimates for the uncertainty in the system state. Stochastic differential equations are often used to mathematically model the underlying system. The Kusuoka-Lyons-Victoir (KLV) approach is a higher order particle method for approximating the weak solution of a stochastic differential equation that uses a weighted set of scenarios to approximate the evolving probability distribution to a high order of accuracy. The algorithm can be performed by integrating along a number of carefully selected bounded variation paths and the iterated application of the KLV method has a tendency for the number of particles to increase. Together with local dynamic recombination that simplifies the support of discrete measure without harming the accuracy of the approximation, the KLV method becomes eligible to solve the filtering problem for which one has to maintain an accurate description of the ever-evolving conditioned measure. Besides the alternate application of the KLV method and recombination for the entire family of particles, we make use of the smooth nature of likelihood to lead some of the particles immediately to the next observation time and to build an algorithm that is a form of automatic high order adaptive importance sampling. We perform numerical simulations to evaluate the efficiency and accuracy of the proposed approaches in the example of the linear stochastic differential equation driven by three independent Brownian motions. Our numerical simulations show that, even when the sequential Monte-Carlo method poorly performs, the KLV method and recombination can together be used to approximate higher order moments of the filtering solution in a moderate dimension with high accuracy and efficiency.

**1. Introduction.** Filtering is an approach for calculating the probability distribution of an evolving system in the presence of noisy observations. The problem has many significant and practical applications in science and engineering, for example navigational and guidance systems, radar track-

---

Primary 60G35; secondary 65D99

*Keywords and phrases:* Bayesian statistics, particle filter, cubature on Wiener space, recombination

ing, sonar ranging, satellite and airplane orbit determination, the spread of hazardous plumes or pollutants, prediction of weather and climate in atmosphere-ocean dynamics [16, 15, 18, 14, 11, 1, 12, 10]. If both the underlying system and the observation process satisfy linear equations, the solution of the filtering problem can be obtained from the Kalman filter [16, 15]. For nonlinear filtering in finite dimension, there occasionally exist analytic solutions but the results are too narrow in applicability [2]. As a result, a number of numerical schemes that use a discrete measure, i.e., collection of weighted Dirac masses, for the approximation of the conditioned measure have been developed [12, 10, 8].

When the underlying dynamics is a continuous process and the associated observation is intermittent in time, one approach to filtering is to make a prediction to quantify uncertainty and then to update this prediction to incorporate data in a sequential fashion. The prediction step corresponds to solving the Kolmogorov forward equation when the system is driven by Brownian motion. For the numerical integration of a stochastic differential equation, the sequential Monte-Carlo method uses sampling from a random vector whose distribution agrees with the law of the truncated strong Taylor expansion of the solution of an Ito diffusion. The algorithm usually gives lower order strong convergence of the probability distribution [17].

Instead of simulating Wiener measure as in the sequential Monte-Carlo method, the KLV method at the path level replaces Brownian motion by a weighted combination of bounded variation paths while making sure that expectations of the iterated integrals with respect to these two measures on Wiener space agree up to a certain degree. Then the particles are deterministically pushed forward along the paths to yield a weighted discrete measure. The KLV method is of higher order with effective and transparent error bounds obtained from the Stratonovich-Taylor expansion of the solution of a stochastic differential equation [26].

It is intrinsic to the KLV method that the number of particles increases when the algorithm is iterated. Therefore its successive application without an efficient suppression of the growth of the number of particles cannot be used to filter the ever-evolving dynamics. Given a family of test functions, one can replace the original discrete measure by a simpler measure with smaller support whose integrations against these test functions agree with those against the original measure. Recombination achieves the reduction of particles in this way using the polynomials as test functions [23]. One advantage of recombination is its local applicability in space. Therefore one can divide the set of particles into a number of disjoint subsets and recombine each clustered discrete measure separately, a process which we call the

patched recombination. The dynamic property of patched recombination, if an efficient classification method is provided, leads to a competitive high order reduction algorithm whose error bound can be obtained from the Taylor expansion of the test function.

One can use the alternate application of the KLV method and patched recombination as an algorithm for the prediction step in filtering. However the cost of this non adaptive method would become extremely high particularly in high dimension. In this paper we modify the algorithm to reduce the computational effort. More precisely, we exploit the internal smoothness of the likelihood to allow some particles to immediately leap to the next observation time provided the support of the resulting measure is far from the observational data. Applying bootstrap reweighting to discrete measures for the updating step, our solution of the filtering problem is consistent with Bayesian statistics.

It is very important to use a good example to examine the performance of the algorithm we have developed. We choose a forward model and observation process for which the analytic solution of the filtering problem is known and use this to measure the accuracy of our approximations. Unlike filtering in practice where the data is determined by a realization of the random process and the observation noise, we arbitrarily fix the observational data to study cases ranging from normal to exceptional and to rare event. This setting is admittedly somewhat artificial however it is carefully designed in order to find the parameter regimes where our approach outperforms Monte-Carlo methods and eventually turns out to be extremely helpful for a deeper understanding of the filtering problem.

The paper is organized as follows. In section 2, we introduce the Bayesian filter. In section 3, we describe a prototypical sequential Monte-Carlo algorithm and its variant. Section 4 defines the patched particle filter and the adaptive patched particle filter. In section 5, we discuss the implementation of the KLV method. Numerical simulations are performed in section 6 and concluding discussions are in section 7.

**2. Bayesian filter.** Suppose that the  $N$ -dimensional underlying Markov process  $X(t), t \in \mathbb{R}^+ \cup \{0\}$ , and the  $N'$ -dimensional observation process  $Y_n, n \in \mathbb{N} \setminus \{0\}$ , associated with  $X_n = X(n \times T)$  are given, for some inter-observation time  $T > 0$ . Let  $Y_{1:n'} \equiv \{Y_1, \dots, Y_{n'}\}$  be the path of the observation process and  $y_{1:n'} \equiv \{y_1, \dots, y_{n'}\}$  be a generic point in the space of paths. We define the measure of the conditioned variable  $X_n | Y_{1:n'}$  by  $\pi_{n|n'}(dx_n) = \mathbb{P}(X_n \in dx_n | Y_{1:n'} = y_{1:n'})$ . Given  $\pi_{0|0}$  which is the law of  $X(0)$ , filtering aims to find  $\pi_{n|n}$  for all  $n \geq 1$ .

This intermittent data assimilation problem can be solved by the alternate application of the prediction, to obtain the prior  $\pi_{n|n-1}$  from  $\pi_{n-1|n-1}$ , and the updating, to obtain the posterior  $\pi_{n|n}$  from  $\pi_{n|n-1}$ . If the transition kernel  $K(dx_n|x_{n-1})$  and the likelihood function  $g(y_n|x_n)$ , satisfying

$$\begin{aligned}\mathbb{P}(X_n \in A | X_{n-1} = x_{n-1}) &= \int_A K(dx_n|x_{n-1}), \\ \mathbb{P}(Y_n \in B | X_n = x_n) &= \int_B g(y_n|x_n) dy_n,\end{aligned}$$

for all  $A \in \mathcal{B}(\mathbb{R}^N)$ , the Borel  $\sigma$ -algebra, and  $B \in \mathcal{B}(\mathbb{R}^{N'})$ , are given, the prediction and the updating are achieved by

$$(2.1) \quad \pi_{n|n-1}(dx_n) = \int K(dx_n|x_{n-1})\pi_{n-1|n-1}(dx_{n-1}),$$

$$(2.2) \quad \pi_{n|n}(dx_n) = \frac{g(y_n|x_n)\pi_{n|n-1}(dx_n)}{\int g(y_n|x_n)\pi_{n|n-1}(dx_n)},$$

respectively. Eq. (2.2) is Bayes' rule and the recursive scheme (2.1), (2.2) is called a Bayesian filter.

### 3. Particle filtering.

3.1. *Weak approximation.* The closed form of  $\pi_{n|n'}$  is in general not available. In many cases the essential properties of a probability measure we are interested can accurately be described by the expectation of test functions. If the class of test functions is specified, we can replace the original measure with a simpler measure that integrates the test functions correctly and hence still keeps the right properties of the original measure. Therefore efforts have been devoted to weakly approximating  $\pi_{n|n'}$  by finding an efficient way to compute  $\mathbb{E}(f(X_n)|Y_{1:n'}) = \int f(x_n)\pi_{n|n'}(dx_n)$  accurately for a sufficiently large class of  $f : \mathbb{R}^N \rightarrow \mathbb{R}$ . We mention that the class of test functions is not given in the filtering problem. Their choice is quite critical as it affects the notion of an optimal algorithm and controls the detailed description of the conditioned measure.

One of the methodologies for the weak approximation is to employ *particles* whose locations and weights characterize the approximation of the conditioned measure. More precisely, a particle filter is a recursive algorithm that produces

$$(3.1) \quad \pi_{n|n'}^{\text{PF}} = \sum_{i=1}^{M_{n|n'}} \lambda_{n|n'}^i \delta_{x_{n|n'}^i}$$

approximating  $\pi_{n|n'}$ , where  $\delta_x$  denotes the Dirac mass centered at  $x$ . One approximates  $(\pi_{n|n'}, f)$  by  $(\pi_{n|n'}^{\text{PF}}, f) = \sum_{i=1}^{M_{n|n'}} \lambda_{n|n'}^i f(x_{n|n'}^i)$  where the notation  $(\pi, f) = \int f(x)\pi(dx)$  is used.

**3.2. Sequential Monte-Carlo method.** Particle approximation is widely used in Monte-Carlo methods. We here introduce the bootstrap filter or sampling importance resampling (SIR) suggested in [12] and the sequential importance sampling (SIS) algorithm [24, 31, 9]. The number of particles do not have to be equal in each step, but we here fix it by  $M_{n|n'} = M$  for simplicity.

**3.2.1. Bootstrap filter or sampling importance resampling (SIR).** The prediction is achieved by using  $(\pi_{n|n-1}, f) = (\pi_{n-1|n-1}, Kf)$  from Eq. (2.1). Given the empirical measure  $\pi_{n-1|n-1}^{\text{SIR}} = \frac{1}{M} \sum_{i=1}^M \delta_{x_{n-1|n-1}^i}$  approximating  $\pi_{n-1|n-1}$ , one performs independent and identically distributed (i.i.d.) sampling  $\tilde{x}_{n|n-1}^i$  drawn from  $K(dx_n|x_{n-1|n-1}^i)$ . Then the discrete measure  $\pi_{n|n-1}^{\text{SIR}} = \frac{1}{M} \sum_{i=1}^M \delta_{\tilde{x}_{n|n-1}^i}$  is distributed according to  $\pi_{n|n-1}$ .

For the updating, Eq. (2.2) implies that  $(\pi_{n|n}, f) = (\pi_{n|n-1}, fg^{y_n}) / (\pi_{n|n-1}, g^{y_n})$  where the notation  $g^{y_n}(\cdot) \equiv g(y_n|\cdot)$  is used. We are led to define the bootstrap reweighting operator

$$(3.2) \quad \text{REW} \left( \sum_{i=1}^n \kappa_i \delta_{x^i}, g^{y_n} \right) \equiv \frac{\sum_{i=1}^n \kappa_i g^{y_n}(x^i) \delta_{x^i}}{\sum_{i=1}^n \kappa_i g^{y_n}(x^i)}.$$

Then  $\bar{\pi}_{n|n}^{\text{SIR}} = \text{REW} \left( \pi_{n|n-1}^{\text{SIR}}, g^{y_n} \right)$  is distributed according to  $\pi_{n|n}$ .

In order to prevent degeneracy in the weights, one approximates the weighted discrete measure  $\bar{\pi}_{n|n}^{\text{SIR}}$  by an equally weighted discrete measure [8]. Random resampling performs  $M$  independent samples  $\{x_{n|n}^i\}_{i=1}^M$  from  $\bar{\pi}_{n|n}^{\text{SIR}}$ . This process can introduce a large Monte-Carlo variation and work has been done to reduce the variance [4, 7]. The resulting discrete measure  $\pi_{n|n}^{\text{SIR}} = \frac{1}{M} \sum_{i=1}^M \delta_{x_{n|n}^i}$  is distributed according to  $\pi_{n|n}$ .

The SIR algorithm can be displayed by

$$(3.3) \quad \pi_{n-1|n-1}^{\text{SIR}} \mapsto \pi_{n|n-1}^{\text{SIR}} \Rightarrow \bar{\pi}_{n|n}^{\text{SIR}} \rightarrow \pi_{n|n}^{\text{SIR}}$$

where the notation  $\mapsto$  is used for moving particles forward in time,  $\Rightarrow$  for reweighting and  $\rightarrow$  for random resampling. The algorithm is very intuitive and straightforward to implement. Further, it produces an approximation

that converges toward to the true posterior as the number of particles increases [5]. However SIS might be inefficient when  $\pi_{n|n-1}^{\text{SIR}}$  is far from  $\pi_{n|n}$  in the sense that bootstrap reweighting generates importance weights with a high variance. The following SIS algorithm modifies SIR to get around this problem.

**3.2.2. Sequential importance sampling (SIS).** Given the unweighted measure  $\pi_{n-1|n-1}^{\text{SIS}} = \frac{1}{M} \sum_{i=1}^M \delta_{x_{n-1|n-1}^i}$  that approximates  $\pi_{n-1|n-1}$ , one performs i.i.d. sampling  $\tilde{x}_{n|n-1}^i \sim \tilde{K}(dx_n|x_{n-1|n-1}^i, y_n)$  instead of  $\bar{x}_{n|n-1}^i \sim K(dx_n|x_{n-1|n-1}^i)$ . Here the new transition kernel  $\tilde{K}$  can depend on  $y_n$  and should be chosen in a way that the distribution of  $\pi_{n|n-1}^{\text{SIS}} = \frac{1}{M} \sum_{i=1}^M \delta_{\tilde{x}_{n|n-1}^i}$  is closer to  $\pi_{n|n}$  than  $\pi_{n|n-1}^{\text{SIR}}$  in the above-mentioned sense [9].

Note that  $\pi_{n|n-1}^{\text{SIS}}$  is not distributed according to  $\pi_{n|n-1}$ . To account for the effect of this discrepancy, the expression

$$(3.4) \quad \begin{aligned} & \mathbb{P}(X_{n-1} \in dx_{n-1}, X_n \in dx_n | Y_{1:n} = y_{1:n}) \\ &= \frac{w(x_{n-1}, x_n, y_n) \tilde{K}(dx_n|x_{n-1}, y_n) \pi_{n-1|n-1}(dx_{n-1})}{\int w(x_{n-1}, x_n, y_n) \tilde{K}(dx_n|x_{n-1}, y_n) \pi_{n-1|n-1}(dx_{n-1})} \end{aligned}$$

where

$$w(x_{n-1}, x_n, y_n) \propto \frac{g(y_n|x_n) K(dx_n|x_{n-1})}{\tilde{K}(dx_n|x_{n-1}, y_n)}$$

is used. Replacing  $\tilde{K}(dx_n|x_{n-1}) \pi_{n-1|n-1}(dx_{n-1})$  in Eq. (3.4) by its empirical approximation and integrating over  $x_{n-1}$ , one obtains  $\tilde{\pi}_{n|n}^{\text{SIS}} = \sum_{i=1}^M w^i \delta_{\tilde{x}_{n|n-1}^i}$  where  $w^i \propto w(x_{n-1|n-1}^i, \tilde{x}_{n|n-1}^i, y_n)$  that is distributed according to  $\pi_{n|n}$ . Random sampling from  $\tilde{\pi}_{n|n}^{\text{SIS}}$  yields the empirical measure  $\pi_{n|n}^{\text{SIS}}$ .

If  $\tilde{K}(dx_n|x_{n-1}, y_n)$  and  $w(x_{n-1}, x_n, y_n)$  have better theoretical properties than  $K(dx_n|x_{n-1})$  and  $g(y_n|x_n)$  such as better mixing properties of  $\tilde{K}(dx_n|x_{n-1}, y_n)$  or flatter likelihood  $w(x_{n-1}, x_n, y_n)$ , then the algorithm will outperform. Because one needs to integrate an evolution equation of a Markov process with transition kernel  $\tilde{K}$  in any practical implementation, designing efficient particle filtering methods is equivalent to finding an appropriate dynamic model that has good theoretical properties while keeping the same filtering distributions. In the numerical simulations performed in [36], the SIS algorithm

$$(3.5) \quad \pi_{n-1|n-1}^{\text{SIS}} \mapsto \pi_{n|n-1}^{\text{SIS}} \Rightarrow \tilde{\pi}_{n|n}^{\text{SIS}} \rightarrow \pi_{n|n}^{\text{SIS}}$$

uses far fewer particles than SIR to achieve a given degree of accuracy.

In the subsequent section, we develop two non Monte-Carlo particle filtering algorithms that retains the strengths and mitigates the weaknesses of the SIR and SIS methods.

**4. Introducing cubature to filtering.** Suppose that a random vector  $X(t) \in \mathbb{R}^N$  evolves according to a Stratonovich stochastic differential equation (SDE)

$$(4.1) \quad dX(t) = V_0(X(t)) dt + \sum_{i=1}^d V_i(X(t)) \circ dW_i(t)$$

where  $\{V_i \in C_b^\infty(\mathbb{R}^N, \mathbb{R}^N)\}_{i=0}^d$  is a family of smooth vector fields from  $\mathbb{R}^N$  to  $\mathbb{R}^N$  with bounded derivatives of all orders, and  $W = (W_1, \dots, W_d)$  denote a set of Brownian motions, independent of one another. The noisy observations  $Y_n$  associated with  $X_n = X(n \times T)$  are given by

$$(4.2) \quad Y_n = \varphi(X_n) + \eta_n, \quad \eta_n \sim \mathcal{N}(0, R_n)$$

where  $\varphi \in C_b^\infty(\mathbb{R}^N, \mathbb{R}^{N'})$  and realizations of the noise  $\eta_n$  are i.i.d. random vectors in  $\mathbb{R}^{N'}$ .

The two main ingredients in developing the patched particle filter (PPF) and the adaptive patched particle filter (APPF) to solve the filtering problem (4.1), (4.2) are cubature on a finite dimensional space and cubature on (infinite dimensional) Wiener space. Both are discrete measures and defined in subsection 4.1 and subsection 4.2, respectively. We describe the KLV method in subsection 4.2 and the patched recombination in subsection 4.3. Subsection 4.4 provides the PPF algorithm together with error estimates and subsection 4.5 defines the APPF.

4.1. *Cubature on a finite dimensional space.* Let  $\nu$  be a (possibly unnormalized) measure on  $\mathbb{R}^N$ . A discrete measure  $\hat{\nu}^{(r)} = \sum_{j=1}^{n_r} w_j \delta_{y^j}$  is called a cubature (quadrature when  $N = 1$ ) of degree  $r$  with respect to  $\nu$ , if  $(\nu, q)$  equals  $(\hat{\nu}^{(r)}, q) = \sum_{j=1}^{n_r} w_j q(y^j)$  for all polynomials  $q$  whose total degree is less than or equal to  $r$ . It is proved that a cubature  $\hat{\nu}^{(r)}$  with respect to an arbitrary positive measure  $\nu$  satisfying  $n_r \leq \binom{N+r}{r}$  exists [32].

Importantly, an error bound of  $(\nu, F) - (\hat{\nu}^{(r)}, F) \equiv (\nu - \hat{\nu}^{(r)}, F)$  for a smooth function  $F : \mathbb{R}^N \rightarrow \mathbb{R}$  can be obtained from the Taylor expansion. The value of  $F$  at  $x = (x_1, \dots, x_N)$  is written as

$$(4.3) \quad F(x) = \sum_{|\alpha| \leq r} \frac{D^\alpha F(x_0)}{\alpha!} (x - x_0)^\alpha + R^r(x, x_0, F)$$

where  $\alpha \equiv (\alpha_1, \dots, \alpha_N)$ ,  $|\alpha| \equiv \alpha_1 + \dots + \alpha_N$ ,  $\alpha! \equiv \alpha_1! \dots \alpha_N!$ ,  $D^\alpha \equiv \partial x_1^{\alpha_1} \dots \partial x_N^{\alpha_N}$ ,  $x^\alpha \equiv x_1^{\alpha_1} \dots x_N^{\alpha_N}$  and

$$(4.4) \quad R^r(x, x_0, F) = \sum_{|\alpha|=r+1} \frac{D^\alpha F(x^*)}{\alpha!} (x - x_0)^\alpha$$

for some  $x^* \in \mathbb{R}^N$ . If the support of  $\nu$  is in a closed ball of center  $x_0$  and radius  $u$ , denoted by  $B(x_0, u)$ , then we have

$$(4.5) \quad \begin{aligned} |(\nu - \widehat{\nu}^{(r)}, F)| &= |(\nu - \widehat{\nu}^{(r)}, R^r)| \leq 2(\nu, 1) \|R^r\|_{L_\infty(B(x_0, u))} \\ &\leq \frac{Cu^{r+1}}{(r+1)!} \sup_{|\alpha|=r+1} \|D^\alpha F\|_{L_\infty(B(x_0, u))}. \end{aligned}$$

Here and after,  $C$  denotes a constant. Eq. (4.5) reveals that cubature on a finite dimensional space is an approach for numerical integration of functions on finite dimensional space with a clear error bound.

Let  $f$  be a function defined on a closed set  $B \subseteq \mathbb{R}^N$ . We call  $f$  by a Lipschitz function if there exists a constant  $C'$ ,  $\{f^i\}_{i=0}^{\rho-1}$  ( $f^0 = f$ ) and  $R_i : B \times B \rightarrow \mathbb{R}$  such that  $|f| \leq C'$ ,  $|f^i| \leq C'$ ,  $f^i(x) = \sum_{l=0}^{\rho-1-i} f^{i+l}(y)(x-y)^l/l! + R_i(x, y)$  and  $|R_i(x, y)| \leq C' \|x-y\|^{\rho-i}$ . The smallest  $C'$  for which the inequalities hold for all integer  $i \in [0, \rho)$  is called the Lipschitz norm of  $f$ , denoted by  $\|f\|_{\text{Lip}(\rho)}$ . Note that  $f$  is defined locally, but can be extended to the entire space by the Whitney theorem [33]. Eq. (4.5) implies

$$(4.6) \quad |(\nu - \widehat{\nu}^{(r)}, F)| \leq \frac{Cu^{r+1}}{(r+1)!} \|F\|_{\text{Lip}(r+1)}.$$

Note that  $f$  is Lipschitz continuous if and only if  $\|f\|_{\text{Lip}(1)}$  is finite.

4.2. *Cubature on Wiener space and the KLV method.* Consider the iterated integral with respect to  $W = (W_1, \dots, W_d)$ ,

$$\mathcal{J}_{0,T}^I(\circ W) \equiv \int_{0 < t_1 < \dots < t_l < T} \circ dW_{i_1}(t_1) \dots \circ dW_{i_l}(t_l),$$

and the iterated integral with respect to a continuous path of bounded variation  $\omega_T = (\omega_{T,1}, \dots, \omega_{T,d}) : [0, T] \rightarrow \mathbb{R}^d$ ,

$$\mathcal{J}_{0,T}^I(\omega_T) \equiv \int_{0 < t_1 < \dots < t_l < T} d\omega_{T, i_1}(t_1) \dots d\omega_{T, i_l}(t_l),$$

where the notations  $W_0(t) = t$ ,  $\omega_{T,0}(t) = t$  and  $I = (i_1, \dots, i_l) \in \{0, \dots, d\}^l$  are used. Recall that Wiener space  $C_0^0([0, T], \mathbb{R}^d)$  is the set of continuous



functions starting at zero. We define a discrete measure  $\mathbb{Q}_T^m = \sum_{j=1}^{n_m} \lambda_j \delta_{\omega_T^j}$  supported on continuous paths of bounded variation to be a cubature on Wiener space of degree  $m$  with respect to the Wiener measure  $\mathbb{P}$ , if the equation

$$(4.7) \quad \begin{aligned} \mathbb{E}_{\mathbb{P}} (\mathcal{J}_{0,T}^I(\circ W)) &= \mathbb{E}_{\mathbb{Q}_T^m} (\mathcal{J}_{0,T}^I(\circ W)) \\ &= \sum_{j=1}^{n_m} \lambda_j \mathcal{J}_{0,T}^I(\omega_T^j) \end{aligned}$$

holds for all  $I$  satisfying  $\|I\| \equiv l + \text{card}\{j, i_j = 0\} \leq m$ . The existence of  $\mathbb{Q}_T^m$  with  $n_m \leq \text{card}\{I : \|I\| \leq m\}$  is proved in [26].

Similarly with the case of cubature on  $\mathbb{R}^N$ , cubature on Wiener space can be used to approximate  $\mathbb{E}_{\mathbb{P}}(f(X_T^x))$  for the random process  $X_t^x$  in  $N$  dimension satisfying

$$(4.8) \quad dX_t^x = V_0(X_t^x) dt + \sum_{i=1}^d V_i(X_t^x) \circ dW_i(t)$$

and  $X_0^x = x$ . The expectation of  $f(X_T^x)$  against Wiener measure can be viewed as an integral with respect to infinite dimensional Wiener space.

Let  $t \mapsto X_t^{x, \omega_\Delta^j}$  for  $t \in [0, \Delta]$  be the deterministic process satisfying

$$(4.9) \quad dX_t^{x, \omega_\Delta^j} = \sum_{i=0}^d V_i(X_t^{x, \omega_\Delta^j}) d\omega_{\Delta, i}^j(t)$$

and  $X_0^{x, \omega_\Delta^j} = x$ . The ordinary differential equations (ODEs) of Eq. (4.9) are obtained from replacing the Brownian motions  $W$  in Eq. (4.8) by the bounded variation path  $\omega_\Delta^j$ . The measure  $\sum_{j=1}^{n_m} \lambda_j \delta_{X_T^{x, \omega_\Delta^j}}$  on  $\mathbb{R}^N$  is called the cubature approximation of the law of  $X_T^x$  at the path level. Note that this discrete measure obtained from solving ODEs is in general not a cubature with respect to the law of  $X_T^x$ .

An error estimate for the weak approximation of this particle method can be derived from the Stratonovich-Taylor expansion of a smooth function  $f$ ,

$$(4.10) \quad f(X_T^x) = \sum_{\|I\| \leq m} V_I f(x) \mathcal{J}_{0,T}^I(\circ W) + R_m(x, T, f)$$

where the remainder  $R_m(x, T, f)$  satisfies

$$(4.11) \quad \sup_{x \in \mathbb{R}^N} \sqrt{\mathbb{E}_{\mathbb{P}}(R_m(x, T, f)^2)} \leq C \sum_{i=m+1}^{m+2} T^{i/2} \sup_{\|I\|=i} \|V_I f\|_\infty$$

for a constant  $C$  depending on  $d$  and  $m$  [17]. Here the vector field  $V_i = (V_{i,1}, \dots, V_{i,N})$  is used as the differential operator  $V_i \equiv \sum_{j=1}^N V_{i,j} \partial x_j$  and  $V_I$  denotes  $V_{i_1} \cdots V_{i_k}$ . Note that  $\mathcal{J}_{0,T}^I(\circ W)$  works as a basis of the expansion in Eq. (4.10) analogous to the monomial in Eq. (4.3).

The process  $R_m(x, T, f)$  further satisfies

$$(4.12) \quad \sup_{x \in \mathbb{R}^N} \mathbb{E}_{\mathbb{Q}_T^m}(|R_m(x, T, f)|) \leq C \sum_{i=m+1}^{m+2} T^{i/2} \sup_{\|I\|=i} \|V_I f\|_\infty$$

for a constant  $C$  depending on  $d$ ,  $m$  and  $\mathbb{Q}_1^m$  [26]. Then the error bound of the cubature approximation at the path level is given by

$$(4.13) \quad \begin{aligned} & \sup_{x \in \mathbb{R}^N} \left| \mathbb{E}_{\mathbb{P}}(f(X_T^x)) - \sum_{j=1}^{n_m} \lambda_j f(X_T^{x, \omega_T^j}) \right| \\ &= \| (P_T - Q_T^m) f \|_\infty \leq C \sum_{i=m+1}^{m+2} T^{i/2} \sup_{\|I\|=i} \|V_I f\|_\infty \end{aligned}$$

for smooth  $f$ , from Eq. (4.7) and Eqs. (4.10), (4.11), (4.12). The operators  $P_T$  and  $Q_T^m$  are defined by  $P_T f(x) \equiv \mathbb{E}_{\mathbb{P}}(f(X_T^x))$  and  $Q_T^m f(x) \equiv \mathbb{E}_{\mathbb{Q}_T^m}(f(X_T^x))$ .

The algorithm was developed by Lyons, Victoir [26], following the work of Kusuoka [19, 21], so it is referred to as the KLV method. Eq. (4.13) leads to define

$$(4.14) \quad \text{KLV}^{(m)} \left( \sum_{i=1}^n \kappa_i \delta_{x^i}, \Delta \right) \equiv \sum_{i=1}^n \sum_{j=1}^{n_m} \kappa_i \lambda_j \delta_{X_\Delta^{x^i, \omega_\Delta^j}}$$

that may be interpreted as a Markov operator acting on discrete measures on  $\mathbb{R}^N$ .

In the following, assume  $T \in (0, 1)$  for simplicity. One may take a higher degree  $m$  to achieve a given degree of accuracy in Eq. (4.13). Another method to improve the accuracy of the particle approximation is a successive application of the KLV operator. Let  $\mathcal{D} = \{0 = t_0 < t_1 < \cdots < t_k = T\}$  be a partition of  $[0, T]$  with  $s_j = t_j - t_{j-1}$ . Instead of  $Q_T^m f(x) = (\text{KLV}^{(m)}(\delta_x, T), f)$ , the value of  $P_T f(x) = P_{s_1} P_{s_2} \cdots P_{s_k} f(x)$  can accurately be approximated by a multiple step algorithm  $Q_{s_1}^m Q_{s_2}^m \cdots Q_{s_k}^m f(x)$ .

Given a discrete measure  $\mu^0$ , we define a sequence of discrete measure by

$$(4.15) \quad \begin{aligned} \Phi_{\mathcal{D}}^{m,0}(\mu^0) &= \mu^0, \\ \Phi_{\mathcal{D}}^{m,j}(\mu^0) &= \text{KLV}^{(m)}(\Phi_{\mathcal{D}}^{m,j-1}(\mu^0), s_j) \quad 1 \leq j \leq k \end{aligned}$$

that can be viewed as Markov chain. The inequality

$$\begin{aligned}
& \left| P_T f(x) - (\Phi_{\mathcal{D}}^{m,k}(\delta_x), f) \right| \\
&= \left| \sum_{j=1}^k \left( \Phi_{\mathcal{D}}^{m,j-1}(\delta_x), P_{T-t_{j-1}} f \right) - \left( \Phi_{\mathcal{D}}^{m,j}(\delta_x), P_{T-t_j} f \right) \right| \\
&= \left| \sum_{j=1}^k \left( \Phi_{\mathcal{D}}^{m,j-1}(\delta_x), (P_{s_j} - Q_{s_j}^m) P_{T-t_j} f \right) \right| \\
(4.16) \quad & \leq \sum_{j=1}^k \| (P_{s_j} - Q_{s_j}^m) P_{T-t_j} f \|_{\infty}
\end{aligned}$$

obtained from the Markovian property of the KLV operator shows that the total error of the repeated KLV application is bounded above by the sum of the errors over the subintervals in the partition. Applying Eq. (4.13) to estimate the upper bound of Eq. (4.16), we need  $P_{T-t_j} f$  to be smooth and it is true provided  $f$  is smooth. In this case, the error bound

$$\sup_{x \in \mathbb{R}^N} \left| P_T f(x) - (\Phi_{\mathcal{D}}^{m,k}(\delta_x), f) \right| \leq C \sum_{i=m+1}^{m+2} \sum_{j=1}^k s_j^{i/2} \sup_{\|I\|=i} \| V_I P_{T-t_j} f \|_{\infty}$$

is obtained from Eqs. (4.13), (4.16).

The case of Lipschitz continuous  $f$  is of particular interest because  $P_t f$  is indeed smooth in the direction of  $\{V_i\}_{i=0}^d$  with additional conditions for these vector fields. In the following we assume  $\{V_i\}_{i=0}^d$  satisfy the UFG and V0 conditions (see [6]), then  $P_t f$  is smooth for a Lipschitz continuous  $f$  and the regularity estimate

$$(4.17) \quad \| V_I P_t f \|_{\infty} \leq \frac{C}{t^{(\|I\|-1)/2}} \| \nabla f \|_{\infty}$$

holds for all  $t \in (0, 1]$ , where  $C$  is a constant independent of  $f$  [22, 20]. Combining Eqs. (4.13), (4.16) and Eq. (4.17), we obtain an error estimate for the KLV method in terms of the gradient of  $f$ ,

$$\begin{aligned}
(4.18) \quad & \sup_{x \in \mathbb{R}^N} \left| P_T f(x) - (\Phi_{\mathcal{D}}^{m,k}(\delta_x), f) \right| \\
& \leq C \| \nabla f \|_{\infty} \left( s_k^{1/2} + \sum_{i=m+1}^{m+2} \sum_{j=1}^{k-1} \frac{s_j^{i/2}}{(T-t_j)^{(i-1)/2}} \right)
\end{aligned}$$

for the Lipschitz continuous  $f$ , where  $C$  is a constant independent of  $k$ . Here the final term in the upper bound of Eq. (4.16) is estimated by  $\|(P_{s_k} - Q_{s_k}^m)f\|_\infty \leq \|P_{s_k}f - f\|_\infty + \|f - Q_{s_k}^m f\|_\infty \leq Cs_k^{1/2} \|\nabla f\|_\infty$  using the boundedness of  $\{V_i\}_{i=0}^d$ .

**THEOREM 4.1.** *Let  $\mathcal{D}(\gamma) = \{t_j\}_{j=0}^k$  be the Kusuoka partition [19] given by*

$$(4.19) \quad t_j = T \left( 1 - \left( 1 - \frac{j}{k} \right)^\gamma \right)$$

*then the error estimate*

$$(4.20) \quad \sup_{x \in \mathbb{R}^N} \left| P_T f(x) - (\Phi_{\mathcal{D}(\gamma)}^{m,k}(\delta_x), f) \right| \leq C \|\nabla f\|_\infty T^{1/2} k^{-(m-1)/2}$$

*is satisfied for a Lipschitz continuous  $f$  when  $\gamma > m - 1$ .*

Eq. (4.20) is obtained from substituting the non-equidistant time discretization  $\mathcal{D}(\gamma)$  into Eq. (4.18). Using this particular choice of partition ensures that the bound of the KLV error is of high order in the number of iterations  $k$ .

Before concluding this subsection, we here mention that  $u(x, t) \equiv \mathbb{E}_{\mathbb{P}}(f(X_{T-t}^x))$  satisfies the partial differential equation (PDE)

$$(4.21) \quad \begin{aligned} \frac{\partial}{\partial t} u(x, t) &= - \left( V_0 + \frac{1}{2} \sum_{i=1}^d V_i^2 \right) u(x, t), \\ u(x, T) &= f(x). \end{aligned}$$

where  $\{V_i\}_{i=0}^d$  are used as differential operators [37]. Therefore  $P_T f(x)$ , the heat kernel applied to  $f$ , is equal to the solution  $u(x, 0)$  of Eq. (4.21). Due to this concrete relationship between parabolic PDEs and SDEs, one can use any well-known algorithm for the solution of Eq. (4.21) in the prediction step of the filtering problem determined by Eq. (4.1) and Eq. (4.2). However it is very important to note the difference between these two problems. One needs to weakly approximate the law of  $X(T)$ , when  $X(0)$  is given by  $\delta_x$ , that accurately integrate the test function  $f$  for the PDE problem while the filtering problem requires one to approximate the posterior measure of  $X_n | Y_{1:n}$  for all  $n \geq 1$ , for which the test function (and the law of  $X(0)$  as well in practice) is not specified.

4.3. *Local dynamic recombination.* A successive application of KLV operator gives rise to geometric growth of the number of particles in view of Eq. (4.14). Except some cases of PDE problem in which the KLV method can produce an accurate approximation with small number of iterations, this geometric growth of particle number prohibits an application of the KLV method especially for the filtering problem where to maintain an accurate description of the ever-evolving measure with reasonable computational cost is an important issue. It is therefore necessary to add a simplification of the discrete measure to the KLV method as a way to control the number of particles in the approximation between the successive iterations.

Though this simplification problem can be solved by random resampling used in the bootstrap filter, we here apply recombination to efficiently reduce the support of discrete measure (see [23] for the detailed algorithm). The method produces a measure with reduced support which preserves the expectations of the polynomials. In this case, the reduced measure is a cubature on  $\mathbb{R}^N$  with respect to the original measure. Because the measure from the KLV method is used to integrate  $P_t f$  which is smooth for Lipschitz continuous  $f$ , one can use the Taylor expansion for the error estimate.

Instead of using a cubature of higher degree to recombine the entire family of particles all at once, we follow the work in [23] to improve the performance by dividing a given discrete measure into locally supported unnormalized measures and replacing each separated measure by the cubature of lower degree. We believe that this local dynamic recombination is a competitive algorithm with general applications mainly because each reduction can be performed in a parallel manner to save computational time and the error bound from the Taylor approximation is of higher order.

Let  $U = (U_i)_{i=1}^R$  be a collection of balls of radius  $u$  that covers the support of discrete measure  $\mu$  on  $\mathbb{R}^N$ , then one can find unnormalized measures  $(\mu_i)_{i=1}^R$  such that  $\mu = \bigsqcup_{i=1}^R \mu_i$  ( $\mu_i$  and  $\mu_j$  have disjoint support for  $i \neq j$ ) and  $\text{supp}(\mu_i) \subseteq U_i \cap \text{supp}(\mu)$ . In this case, we define the patched recombination operator by

$$(4.22) \quad \text{REC}^{(u,r)}(\mu) \equiv \bigsqcup_{i=1}^R \widehat{\mu}_i^{(r)}$$

where  $\widehat{\mu}_i^{(r)}$  denotes a cubature of degree  $r$  with respect to  $\mu_i$ .

Given a discrete measure  $\mu^0$ , we define a sequence of discrete measure by

$$(4.23) \quad \begin{aligned} \Phi_{\mathcal{D},(u,r)}^{m,0}(\mu^0) &= \mu^0, \\ \widehat{\Phi}_{\mathcal{D},(u,r)}^{m,j-1}(\mu^0) &= \text{REC}^{(u_{j-1}, r_{j-1})} \left( \Phi_{\mathcal{D},(u,r)}^{m,j-1}(\mu^0) \right), \\ \Phi_{\mathcal{D},(u,r)}^{m,j}(\mu^0) &= \text{KLV}^{(m)} \left( \widehat{\Phi}_{\mathcal{D},(u,r)}^{m,j-1}(\mu^0), s_j \right), \end{aligned}$$

for  $1 \leq j \leq k$ . An application of Eq. (4.23) with initial condition  $\delta_x$  yields a weak approximation for the law of  $X_T^x$ . One obtains the estimate

$$(4.24) \quad \begin{aligned} & \left| P_T f(x) - (\Phi_{\mathcal{D},(u,r)}^{m,k}(\delta_x), f) \right| \\ &= \left| \sum_{j=1}^k \left( \widehat{\Phi}_{\mathcal{D},(u,r)}^{m,j-1}(\delta_x), P_{T-t_{j-1}} f \right) - \left( \Phi_{\mathcal{D},(u,r)}^{m,j}(\delta_x), P_{T-t_j} f \right) \right. \\ & \quad \left. + \left( \Phi_{\mathcal{D},(u,r)}^{m,j-1}(\delta_x), P_{T-t_{j-1}} f \right) - \left( \widehat{\Phi}_{\mathcal{D},(u,r)}^{m,j-1}(\delta_x), P_{T-t_{j-1}} f \right) \right| \\ &= \left| \sum_{j=1}^k \left( \widehat{\Phi}_{\mathcal{D},(u,r)}^{m,j-1}(\delta_x), (P_{s_j} - Q_{s_j}^m) P_{T-t_j} f \right) \right. \\ & \quad \left. + \left( \Phi_{\mathcal{D},(u,r)}^{m,j-1}(\delta_x) - \widehat{\Phi}_{\mathcal{D},(u,r)}^{m,j-1}(\delta_x), P_{T-t_{j-1}} f \right) \right| \\ &\leq \sum_{j=1}^k \| (P_{s_j} - Q_{s_j}^m) P_{T-t_j} f \|_\infty \\ & \quad + \sum_{j=0}^{k-1} \left| \left( \Phi_{\mathcal{D},(u,r)}^{m,j}(\delta_x) - \widehat{\Phi}_{\mathcal{D},(u,r)}^{m,j}(\delta_x), P_{T-t_j} f \right) \right| \end{aligned}$$

where the first sum of the upper bound is due to the KLV approximation. The second sum is the error introduced by the recombination

Suppose that  $f$  is Lipschitz continuous. The smoothness of  $P_t f$  leads to

$$(4.25) \quad \begin{aligned} & \sup_{x \in \mathbb{R}^N} \left| \left( \Phi_{\mathcal{D},(u,r)}^{m,j}(\delta_x) - \widehat{\Phi}_{\mathcal{D},(u,r)}^{m,j}(\delta_x), P_{T-t_j} f \right) \right| \\ & \leq C u_j^{r_j+1} \sup_{|\alpha|=r_j+1} \| D^\alpha P_{T-t_j} f \|_\infty \end{aligned}$$

for  $0 \leq j \leq k-1$ , where Eq. (4.5) and the triangle inequality are used. In the following we assume  $\{V_i\}_{i=0}^d$  satisfy the UH condition (see [23, 20]), then there exists a positive integer  $p$  such that

$$(4.26) \quad \sup_{|\alpha|=r+1} \| D^\alpha P_t f \|_\infty \leq C t^{-rp/2} \| \nabla f \|_\infty$$

for all  $t \in (0, 1]$ . Since the UH condition implies the UFG and V0 conditions [6], one obtains

$$(4.27) \quad \begin{aligned} & \sup_{x \in \mathbb{R}^N} \left| P_T f(x) - \left( \Phi_{\mathcal{D}, (u, r)}^{m, k}(\delta_x), f \right) \right| \\ & \leq \left( C_1 \left( s_k^{1/2} + \sum_{i=m+1}^{m+2} \sum_{j=1}^{k-1} \frac{s_j^{i/2}}{(T-t_j)^{(i-1)/2}} \right) \right. \\ & \quad \left. + C_2 \sum_{j=1}^{k-1} \frac{u_j^{r_j+1}}{(T-t_j)^{r_j p/2}} \right) \| \nabla f \|_\infty \end{aligned}$$

from Eqs. (4.18), (4.25). Here  $C_1$  and  $C_2$  are constants.

The recombination error can be controlled by the radius of the ball  $u_j$  and the cubature on  $\mathbb{R}^N$  degree  $r_j$ . By choosing a suitable pair  $(u_j, r_j)$ , one can make the order of the recombination error bound not dominant over the order of the error bound in the KLV method.

**THEOREM 4.2.** *In the case of  $(u_j, r_j) = (s_j^{p/2-a}, \lceil m/p \rceil)$  where  $a = (p-1)/(2(\lceil m/p \rceil + 1))$  ( $\lceil x \rceil$  denotes the smallest integer greater than or equal to  $x$ ) or  $(u_j, r_j) = ((s_j^{m+1}/(T-t_j)^{m-rp})^{1/2(r+1)}, m)$ , the error estimate*

$$(4.28) \quad \sup_{x \in \mathbb{R}^N} \left| P_T f(x) - \left( \Phi_{\mathcal{D}(\gamma), (u, r)}^{m, k}(\delta_x), f \right) \right| \leq C \| \nabla f \|_\infty T^{1/2} k^{-(m-1)/2}$$

is satisfied for a Lipschitz continuous  $f$  when  $\gamma > m - 1$ .

Eq. (4.28) is obtained from substituting the partition defined in Eq. (4.19) into Eq. (4.27). It ensures that the recombination can be used without harming the accuracy of the KLV approximation.

**4.4. Patched particle filter.** Let  $\pi_{n|n'}$  be the law of the conditioned variable  $X_n | Y_{1:n'}$  determined by Eqs. (4.1), (4.2). Let  $\pi_{0|0}^{\text{PPF}}$  be a discrete measure distributed according to the law of  $X_0$ . We define the *patched particle filter (PPF) at the path level* by the recursive algorithm

$$(4.29) \quad \begin{aligned} \pi_{n|n-1}^{\text{PPF}} &= \Phi_{\mathcal{D}, (u, r)}^{m, k}(\pi_{n-1|n-1}^{\text{PPF}}), \\ \pi_{n|n}^{\text{PPF}} &= \text{REW} \left( \pi_{n|n-1}^{\text{PPF}}, g^{y_n} \right), \end{aligned}$$

for  $n \geq 1$ . Recall that the bootstrap reweighting operator REW is defined in Eq. (3.2). The PPF does not require random resampling and therefore no Monte-Carlo variation is introduced. The algorithm can be stated as the following.

1. One breaks the measure into patches and performs recombination for each one.
2. One moves given discrete measure forward in time using the KLV method.
3. One performs data assimilation via bootstrap reweighting at every inter-observation time which might differ from the time step for the numerical integration.
4. One again applies the patched recombination.

Using  $\pi_{n-1|n-1}^{\text{PPF}}$  in place of  $\delta_x$  in Eq. (4.24), an error bound of the prior approximation of the PPF is given by

$$\begin{aligned}
(4.30) \quad \left| (\pi_{n|n-1} - \pi_{n|n-1}^{\text{PPF}}, f) \right| &\leq \left| (\pi_{n-1|n-1}, P_T f) - (\pi_{n-1|n-1}^{\text{PPF}}, P_T f) \right| \\
&\quad + \left| (\pi_{n-1|n-1}^{\text{PPF}}, P_T f) - (\Phi_{\mathcal{D},(u,r)}^{m,k}(\pi_{n-1|n-1}^{\text{PPF}}), f) \right| \\
&\leq \left| (\pi_{n-1|n-1} - \pi_{n-1|n-1}^{\text{PPF}}, P_T f) \right| \\
&\quad + \sum_{j=1}^k \| (P_{s_j} - Q_{s_j}^m) P_{T-t_j} f \|_{\infty} \\
&\quad + \sum_{j=0}^{k-1} \left| \left( \Phi_{\mathcal{D},(u,r)}^{m,j}(\pi_{n-1|n-1}^{\text{PPF}}) - \widehat{\Phi}_{\mathcal{D},(u,r)}^{m,j}(\pi_{n-1|n-1}^{\text{PPF}}), P_{T-t_j} f \right) \right|.
\end{aligned}$$

One can use the same argument with the case of PDE problem to obtain a higher order estimate of the PPF. An error bound of the posterior approximation

$$\begin{aligned}
(4.31) \quad \left| (\pi_{n|n} - \pi_{n|n}^{\text{PPF}}, f) \right| &= \left| \frac{(\pi_{n|n-1}, f g^{y_n})}{(\pi_{n|n-1}, g^{y_n})} - \frac{(\pi_{n|n-1}^{\text{PPF}}, f g^{y_n})}{(\pi_{n|n-1}, g^{y_n})} \right. \\
&\quad \left. + \frac{(\pi_{n|n-1}^{\text{PPF}}, f g^{y_n})}{(\pi_{n|n-1}, g^{y_n})} - \frac{(\pi_{n|n-1}^{\text{PPF}}, f g^{y_n})}{(\pi_{n|n-1}^{\text{PPF}}, g^{y_n})} \right| \\
&\leq \frac{1}{(\pi_{n|n-1}, g^{y_n})} \left| (\pi_{n|n-1} - \pi_{n|n-1}^{\text{PPF}}, f g^{y_n}) \right| \\
&\quad + \frac{\| f \|_{\infty}}{(\pi_{n|n-1}, g^{y_n})} \left| (\pi_{n|n-1} - \pi_{n|n-1}^{\text{PPF}}, g^{y_n}) \right|
\end{aligned}$$

is given in terms of an error estimate of the prior approximation. Eq. (4.30) and Eq. (4.31) implies the higher order weak convergence of the PPF.

The implementation of the PPF requires to specify the time partition and the way of dividing the support of measure into patches. Before presenting



the ones used in our numerical simulations, we build a modification of the PPF.

4.5. *Adaptive patched particle filter.* If we know nothing about the smoothness of the test function or any objective function to integrate, then the accuracy requirement leaves no choice other than to let the cloud of particles increase at an appropriate rate to the observation time and the KLV numerical approach indeed allows that to happen. For truly irregular test functions, the computation would be necessarily expensive. This is no surprise since accurate integration would require exploration of the irregularities.

However in many settings the test function is actually piecewise smooth and the less regular set is of significantly lower dimension than the main part of the smoothness. In this case we can apply the same analysis of smoothing but now we observe that the test function in front of a particular point  $(x, T)$  is actually far smoother than would be the case in general. If it is smooth enough, then we can often use our high order method to go straight to the next observation time from some considerable distance back instead of the step predicted in the worst case which we would otherwise have used to terminate the algorithm.

We build this insight into the practical algorithm. At each application of the KLV operator, the algorithm evaluates the test function directly using a one step prediction to the next observation time and compares this with the evaluation using a two (or three to break certain pathological symmetries) step prediction. If two values agree within the error tolerance, then the particles immediately leap to the next observation time. Otherwise the prediction will follow the original partition.

In terms of accuracy, the approach is pragmatically rather successful because the chances of two or three steps producing consistent answers by chance is essentially negligible. Furthermore, the adaptive switch for which the KLV is employed to move the prediction measure forward but move a part of it straight to the observation time whenever the relevant part of the test function in front of the point is smooth enough has a very significant effect of pruning the computation and speeding up the algorithm due to the reduction of particles to be recombined at each iteration.

This adaptive KLV method is an automated form of high order importance sampling and cannot be applied without a test function. Differently from the PDE problem, the test function is not specified in the filtering problem. In practice we take the likelihood as test function to lead an adaptation.

Recall  $\mathcal{D} = \{0 = t_0 < t_1 < \dots < t_k = T\}$  is a partition of  $[0, T]$  with

$s_j = t_j - t_{j-1}$ . We use the likelihood  $g^{y_n}$  to define the splitting operator acting on a discrete measure  $\mu^{j-1} = \sum_{i=1}^n \kappa_i \delta_{x^i}$  at time  $t_{j-1}$ . Let  $\mu_{i,21}^{j-1} = \text{KLV}(\delta_{x^i}, t_j - t_{j-1})$ ,  $\mu_{i,22}^{j-1} = \text{KLV}(\mu_{i,21}, t_k - t_j)$  and  $\mu_{i,1}^{j-1} = \text{KLV}(\delta_{x^i}, t_k - t_{j-1})$ . Let  $I_\tau$  be the collection of index  $i$  satisfying  $|(\mu_{i,1}^{j-1} - \mu_{i,22}^{j-1}, g^{y_n})| < \tau$ . Then the discrete measure  $\mu^{j-1}$  is the union of two discrete measure  $\mu^{j-1} = \mu^{j-1, < \tau} \sqcup \mu^{j-1, \geq \tau}$  where  $\mu^{j-1, < \tau} = \sum_{i \in I_\tau} \kappa_i \delta_{x^i}$ . For simplicity,  $\mu^{k-1, \geq \tau}$  is defined to be the null set. The process defines the splitting operator

$$(4.32) \quad \text{SPL}^{(\tau)}(\mu^{j-1}, g^{y_n}) \equiv \mu^{j-1, < \tau}$$

for  $1 \leq j \leq k$ .

Define a sequence of discrete measures as follows

$$(4.33) \quad \begin{aligned} \Phi_{\mathcal{D},(u,r),\tau}^{m,0}(\mu^0) &= \mu^0, \\ \widehat{\Phi}_{\mathcal{D},(u,r),\tau}^{m,j-1}(\mu^0) &= \text{REC}^{(u_{j-1}, r_{j-1})} \left( \Phi_{\mathcal{D},(u,r),\tau}^{m,j-1}(\mu^0) \right), \\ \widehat{\Phi}_{\mathcal{D},(u,r),\tau}^{m,j-1, < \tau}(\mu^0) &= \text{SPL}^{(\tau)} \left( \widehat{\Phi}_{\mathcal{D},(u,r),\tau}^{m,j-1}(\mu^0), g^{y_n} \right), \\ \Phi_{\mathcal{D},(u,r),\tau}^{m,j}(\mu^0) &= \text{KLV}^{(m)} \left( \widehat{\Phi}_{\mathcal{D},(u,r),\tau}^{m,j-1, < \tau}(\mu^0), s_j \right). \end{aligned}$$

for  $1 \leq j \leq k$ . Let  $\widehat{\Phi}_{\mathcal{D},(u,r),\tau}^{m,j-1}(\mu^0) = \widehat{\Phi}_{\mathcal{D},(u,r),\tau}^{m,j-1, < \tau}(\mu^0) \sqcup \widehat{\Phi}_{\mathcal{D},(u,r),\tau}^{m,j-1, \geq \tau}(\mu^0)$  and

$$(4.34) \quad \Psi_{\mathcal{D},(u,r),\tau}^{m,j-1,k}(\mu^0) = \text{KLV}^{(m)} \left( \text{KLV}^{(m)} \left( \widehat{\Phi}_{\mathcal{D},(u,r),\tau}^{m,j-1, \geq \tau}(\mu^0), t_j - t_{j-1} \right), T - t_j \right).$$

for  $1 \leq j \leq k-1$ . The *adaptive patched particle filter (APPF) at the path level* is defined by

$$(4.35) \quad \begin{aligned} \pi_{n|n-1}^{\text{APPF}} &= \left( \bigsqcup_{j=1}^{k-1} \Psi_{\mathcal{D},(u,r),\tau}^{m,j-1,k}(\pi_{n-1|n-1}^{\text{APPF}}) \right), \\ &\sqcup \Phi_{\mathcal{D},(u,r),\tau}^{m,k}(\pi_{n-1|n-1}^{\text{APPF}}) \\ \pi_n^{\text{APPF}} &= \text{REW} \left( \pi_{n|n-1}^{\text{APPF}}, g^{y_n} \right), \end{aligned}$$

for  $n \geq 1$ . The algorithm can be stated as the following.

1. One breaks the measure into patches and performs recombination for each one.
2. One splits given discrete measure to lead some of the particles to the next observation time and the rest particles to the next iteration time using the KLV method.

3. One performs data assimilation via bootstrap reweighting at every inter-observation time which might differ from the time step for the numerical integration.
4. One again applies the patched recombination.

We here mention that the likelihood is a natural choice in view of Eq. (4.31) for the filtering problem in which the posterior is of primary interest. We also mention that one can apply  $g^{y^n}$  and  $f g^{y^n}$  simultaneously as the test function for the ADA operator in Eq. (4.33) if one would like to obtain a posterior approximation that accurately integrates  $f$ .

It would be interesting to compare the PPF (4.29) and SIR (3.3), and to compare the APPF (4.35) and SIS (3.5). Both PPF and SIR achieve prior approximations without using the observational data, and subsequently achieve posterior approximations via bootstrap reweighting. In that the observation is used to move particles forward in time, the APPF is very much like the SIS algorithm. However, the APPF does not introduce new dynamics and approximates the prior measure of the given forward model. The way of modifying original algorithm is different but the philosophy is the same - making use of the observational information to lead the particles for an efficient approximation of the posterior.

**5. Practical implementation.** In this section we discuss several issues related to the implementation of the PPF and APPF. Some further considerations of cubature on Wiener space are gathered in subsection 5.1. We make use of the test function to define an adaptive partition (subsection 5.2) and adaptive recombination (subsection 5.3).

5.1. *Cubature on Wiener space continued.* We here study the construction of cubature formula  $Q_T^m$ . Cubature on Wiener space in terms of Lie polynomial is defined and used to develop an approximation based on the autonomous ODEs at flow level.

Let  $\{e_i\}_{i=0}^d$  be the standard basis of  $\mathbb{R} \oplus \mathbb{R}^d$ . Let  $\mathcal{T}$  denote the associative and non-commutative tensor algebra of polynomials generated by  $\{e_i\}_{i=0}^d$ . The exponential and logarithm on  $\mathcal{T}$  are defined by

$$(5.1) \quad \begin{aligned} \exp(a) &\equiv \sum_{i=0}^{\infty} \frac{a^{\otimes i}}{i!}, \\ \log(a) &\equiv \log(a_0) + \sum_{i=1}^{\infty} \frac{(-1)^{i-1}}{i} \left( \frac{a}{a_0} - 1 \right)^{\otimes i}, \end{aligned}$$

where  $a = \sum_I a_I e_I$  and  $e_I = e_{i_1} \otimes \cdots \otimes e_{i_l}$  for a multi-index  $I = (i_1, \dots, i_l) \in$

$\{0, \dots, d\}^l$ . Here  $\otimes$  denotes the tensor product. We define the operators  $\exp^{(m)}(\cdot)$  and  $\log^{(m)}(\cdot)$  by the truncation of Eq. (5.1) to the case  $\|I\| \leq m$ .

We define the signature of a continuous path of bounded variation  $\omega_T : [0, T] \rightarrow \mathbb{R}^d$  by

$$\begin{aligned} \mathcal{S}_{0,T}(\omega_T) &\equiv \sum_{l=0}^{\infty} \int_{0 < t_1 < \dots < t_l < T} d\omega_T(t_1) \otimes \dots \otimes d\omega_T(t_l) \\ &= \sum_I \mathcal{J}_{0,T}^I(\omega_T) e_I \end{aligned}$$

and similarly the signature of a Brownian motion  $W$  by

$$\mathcal{S}_{0,T}(\circ W) \equiv \sum_I \mathcal{J}_{0,T}^I(\circ W) e_I.$$

In view of Eq. (4.7), the definition of cubature on Wiener space of degree  $m$  can be rephrased by

$$(5.2) \quad \mathbb{E}_{\mathbb{P}} \left( \mathcal{S}_{0,T}^{(m)}(\circ W) \right) = \mathbb{E}_{\mathbb{Q}_T^m} \left( \mathcal{S}_{0,T}^{(m)}(\circ W) \right)$$

where  $\mathcal{S}_{0,T}^{(m)}(\cdot)$  is the truncation of  $\mathcal{S}_{0,T}(\cdot)$  to the case  $\|I\| \leq m$ .

Define  $\mathcal{L}$  to be the space of Lie polynomials, i.e., linear combinations of finite sequences of Lie brackets  $[e_i, e_j] = e_i \otimes e_j - e_j \otimes e_i$ . Chen's theorem implies that

$$(5.3) \quad \mathcal{L}_T^j \equiv \log^{(m)}(\mathcal{S}_{0,T}(\omega_T^j))$$

is an element of  $\mathcal{L}$ , i.e., a Lie polynomial. Then the measure  $\tilde{\mathbb{Q}}_T^m = \sum_{j=1}^{n_m} \lambda_j \delta_{\mathcal{L}_T^j}$  supported on Lie polynomials satisfies

$$(5.4) \quad \begin{aligned} \mathbb{E}_{\mathbb{P}} \left( \mathcal{S}_{0,T}^{(m)}(\circ W) \right) &= \mathbb{E}_{\tilde{\mathbb{Q}}_T^m} \left( \exp^{(m)}(\mathcal{L}) \right) \\ &= \sum_{j=1}^{n_m} \lambda_j \exp^{(m)}(\mathcal{L}_T^j). \end{aligned}$$

Conversely, for any Lie polynomials  $\mathcal{L}_T^j$ , there exists continuous bounded variation paths  $\omega_T^j$  whose truncated logarithmic signature is  $\mathcal{L}_T^j$ . Moreover if  $\tilde{\mathbb{Q}}_T^m$  satisfies Eq. (5.4), then  $\mathbb{Q}_T^m$  satisfies Eq. (5.2). Therefore Eq. (5.2) and Eq. (5.4) are equivalent. The discrete measure  $\tilde{\mathbb{Q}}_T^m$  is also defined as cubature on Wiener space.

The expectation of the truncated Brownian signature is

$$(5.5) \quad \mathbb{E}_{\mathbb{P}} \left( \mathcal{S}_{0,1}^{(m)}(\circ W) \right) = \exp^{(m)} \left( e_0 + \frac{1}{2} \sum_{i=1}^d e_i \otimes e_i \right)$$

which is proved in [26]. It is immediate from Eq. (5.5) that cubature formulae on Wiener space for  $m = 2n - 1$  and  $m = 2n$  are equal to one another. A formula  $\{\lambda_j, \mathcal{L}_1^j\}_{j=1}^{n_m}$  satisfying Eq. (5.4) is found when  $m = 3$  and  $m = 5$  for any  $d$  [26]. In some cases of  $m \geq 7$ , cubature formula of Lie polynomial is available when  $d = 1, 2$  (See [13]).

From this  $\tilde{\mathbb{Q}}_1^m$  and Eq. (5.3), one can construct  $\mathbb{Q}_1^m$  (See [26, 13]). It follows from the scaling property of the Brownian motion that  $\omega_{T,0}^j(t) = \omega_{1,0}^j(t)$  and  $\omega_{T,i}^j(t) = \sqrt{T} \omega_{1,i}^j(t/T)$  for  $1 \leq i \leq d$ . The paths define a cubature formula  $\tilde{\mathbb{Q}}_T^m$ . Using  $\mathcal{J}_{0,T}^I(\circ W) \triangleq T^{\|I\|/2} \mathcal{J}_{0,1}^I(\circ W)$  and Eq. (5.3), the scaling of the Lie polynomial is  $\mathcal{L}_T^j = \langle T, \mathcal{L}_1^j \rangle$  where  $\langle t, \sum_I a_I e_I \rangle \equiv \sum_I t^{\|I\|/2} a_I e_I$ . The Lie polynomials define a cubature formula  $\mathbb{Q}_T^m$ .

We next study the approximation based on the flows of autonomous ODEs. It is in fact corresponds to a version of Kusuoka's algorithm [19]. Let  $\Gamma$  denote the algebra homomorphism generated by  $\Gamma(e_i) = V_i$  for  $i = 0, \dots, d$ . For a vector field  $V \in C_b^\infty(\mathbb{R}^N, \mathbb{R}^N)$ , we define the flow  $\text{Exp}(tV)(x) \equiv \xi_t^x$  to be the solution of the ODE  $d\xi_t^x = V(\xi_t^x) dt$  with  $\xi_0^x = x$ . By interchanging the algebra homomorphism  $\Gamma$  with the exponentiation (so far taken in the tensor algebra) we arrive at an approximation operator in which the exponentiation is understood as taking the flow of autonomous ODEs. More precisely, one has

$$\begin{aligned} \mathbb{E}_{\mathbb{P}} \left( \Gamma \left( \mathcal{S}_{0,T}^{(m)}(\circ W) \right) \right) f(x) &= \sum_{j=1}^{n_m} \lambda_j \Gamma \left( \exp^{(m)}(\mathcal{L}_T^j) \right) f(x) \\ &\simeq \sum_{j=1}^{n_m} \lambda_j f \left( \text{Exp} \left( \Gamma(\mathcal{L}_T^j) \right) (x) \right) \end{aligned}$$

using Eq. (5.4). The error introduced when interchanging  $\exp$  and  $\Gamma$  turns out to be of the similar order with the error in the cubature approximation of the path level as shown below.

Formally we define the cubature approximation at the flow level as follows. Let  $t \mapsto X_t^{x, \mathcal{L}_\Delta^j}$  for  $t \in [0, 1]$  be the deterministic process satisfying

$$(5.6) \quad dX_t^{x, \mathcal{L}_\Delta^j} = \Gamma(\mathcal{L}_\Delta^j)(X_t^{x, \mathcal{L}_\Delta^j}) dt$$

and  $X_0^{x, \mathcal{L}^j_\Delta} = x$ . We define the operator

$$(5.7) \quad \widetilde{\text{KLV}}^{(m)} \left( \sum_{i=1}^n \kappa_i \delta_{x^i}, \Delta \right) \equiv \sum_{i=1}^n \sum_{j=1}^{n_m} \kappa_i \lambda_j \delta_{X_1^{x^i, \mathcal{L}^j_\Delta}}$$

and a sequence of discrete measure

$$\begin{aligned} \widetilde{\Phi}_{\mathcal{D}}^{m,0}(\mu^0) &= \mu^0, \\ \widetilde{\Phi}_{\mathcal{D}}^{m,j}(\mu^0) &= \widetilde{\text{KLV}}^{(m)}(\widetilde{\Phi}_{\mathcal{D}}^{m,j-1}(\mu^0), s_j) \end{aligned}$$

for  $1 \leq j \leq k$ .

Let  $\widetilde{Q}_T^m f(x) \equiv (\widetilde{\text{KLV}}^{(m)}(\delta_x, T), f)$  be a flow level cubature approximation, then the Taylor expansions of Eq. (4.9) and Eq. (5.6) lead to

$$(5.8) \quad \|(Q_T^m - \widetilde{Q}_T^m)f\|_\infty \leq C \sum_{m+1 \leq \|I\| \leq 2m} T^{\|I\|/2} \|V_I f\|_\infty$$

for a smooth  $f$ , where  $C$  is a constant depending on  $m$ ,  $d$ ,  $\mathbb{Q}_1^m$  and  $\widetilde{\mathbb{Q}}_1^m$  [19].

**THEOREM 5.1.** *The error estimate*

$$(5.9) \quad \sup_{x \in \mathbb{R}^N} \left| P_T f(x) - (\widetilde{\Phi}_{\mathcal{D}(\gamma)}^{m,k}(\delta_x), f) \right| \leq C \|\nabla f\|_\infty T^{1/2} k^{-(m-1)/2}$$

is satisfied for a Lipschitz continuous  $f$  when  $\gamma > m - 1$ .

Eq. (5.9) is obtained using Eq. (5.8) and demonstrates that for a suitable partition the bounds for the approximation at flow and path level have the same rate of convergence in view of Eq. (4.20). Therefore the path level operator  $\text{KLV}^{(m)}$  can be replaced by the flow level operator  $\widetilde{\text{KLV}}^{(m)}$  without harming the order of accuracy. By doing this to the PPF at the path level, we define the *PPF at the flow level* by the successive algorithm that produces  $\widetilde{\pi}_{n|n-1}^{\text{PPF}}$  and  $\widetilde{\pi}_{n|n}^{\text{PPF}}$ . Furthermore, by replacing  $\text{KLV}^{(m)}$  by  $\widetilde{\text{KLV}}^{(m)}$ , we define the *APPF at the flow level* that produces  $\widetilde{\pi}_{n|n-1}^{\text{APPF}}$  and  $\widetilde{\pi}_{n|n}^{\text{APPF}}$  instead of  $\pi_{n|n-1}^{\text{APPF}}$  and  $\pi_{n|n}^{\text{APPF}}$ .

**5.2. Adaptive partition.** Recall that the regularity estimate of Eq. (4.17) for the Lip(1) function is used to obtain the higher order error bound of Eq. (4.20). It implies that the Kusuoka partition in Eq. (4.19) is suitable to accurately integrate any Lip(1) function.

For a given test function  $f$  that might have different regularity from the Lipschitz continuity, one can make use of the heat kernel  $P_t$  to evolve cloud of particles so that one step error is within a given degree of accuracy, i.e.,

$$(5.10) \quad \| (P_{s_j} - Q_{s_j}^m) P_{T-t_j} f \|_\infty < \epsilon$$

for some  $\epsilon > 0$ . We define an adaptive partition  $\mathcal{D}(\epsilon, f) = \{t_j\}_{j=0}^k$  to be a time discretization for which each  $s_j = t_j - t_{j-1}$  is the supremum among the ones satisfying Eq. (5.10). Because  $P_t f$  becomes smoother as  $t$  increases, the sequence  $\{s_j\}_{j=1}^k$  tends to decrease monotonically, i.e.,  $s_1 \geq s_2 \geq \dots \geq s_k$ . The upper bound of the total error due to the adaptive partition is given by

$$|P_T f(x) - (\Phi_{\mathcal{D}}^{m,k}(\delta_x), f)| < k\epsilon$$

from Eq. (4.16).

In order to find  $\mathcal{D}(\epsilon, f)$ , the smooth function  $P_{T-t_j} f$  has to be approximated. One solution is to compute  $P_{T-t_j} f(z_i)$  for finitely many  $z_i \in \mathbb{R}^N$  (which can be done by using the KLV method or the Monte-Carlo method) and to use the interpolation scheme developed in the scattered data approximation [38].

When  $f$  is a Lipschitz function, adaptive partition can be analyzed by the Lipschitz norm. Note that the inequalities

$$(5.11) \quad \begin{aligned} \| (P_{s_j} - Q_{s_j}^m) P_{T-t_j} f \|_\infty &\leq C s_j^{\frac{m+1}{2}} \sup_{\|I\|=m+1, m+2} \| V_I P_{T-t_j} f \|_\infty \\ &\leq C s_j^{\frac{m+1}{2}} \| P_{T-t_j} f \|_{\text{Lip}(m+2)} \end{aligned}$$

hold from Eq. (4.13) and from the definition of the Lipschitz norm. Suppose that we have the axiom

$$(5.12) \quad \| P_t f \|_{\text{Lip}(\rho')} \leq \frac{K}{t^\alpha} \| f \|_{\text{Lip}(\rho)}$$

where  $K$  and  $\alpha$  are determined by  $\rho$  and  $\rho'$ , which is a generalisation of the regularity estimate of Eq. (4.17) or Eq. (4.26). One can use Eq. (5.11) and Eq. (5.12) to quantify  $s_j$  satisfying Eq. (5.10) in terms of the Lipschitz norm of  $f$ .

5.3. *Adaptive recombination.* Similarly with Eq. (5.10), we consider the condition

$$(5.13) \quad \left| \left( \Phi_{\mathcal{D},(u,r)}^{m,j}(\mu^0) - \widehat{\Phi}_{\mathcal{D},(u,r)}^{m,j}(\mu^0), P_{T-t_j} f \right) \right| < \theta$$

where  $\mu^0 = \delta_x$  for the PDE problem or  $\mu^0 = \pi_{n-1|n-1}^{\text{PPF}}$  for the PPF, given some  $\theta > 0$ . We define the adaptive recombination by the algorithm that uses the maximum value of  $u$ , for fixed recombination degree  $r$ , among the ones satisfying Eq. (5.13). Combining Eq. (5.10) and Eq. (5.13) yields the error bound

$$|P_T f(x) - (\Phi_{\mathcal{D},(u,r)}^{m,k}(\delta_x), f)| < k(\epsilon + \theta)$$

from Eq. (4.24).

The implementation of the adaptive recombination does not require to specify the size of patches: it is enough to keep making the size of patches smaller until Eq. (5.13) is satisfied. The adaptive recombination is useful, particularly in high dimensions, together with the Morton ordering [28]. Instead of balls, the method uses boxes as container of the patched particles.

Assume that the particles are in  $[0.5, 1)^N$ , a box of  $N$  dimension. In double-precision floating-point format, any  $z^i \in [0.5, 1)$  is expressed in terms of  $\{b_j^i\}_{j=1}^{52}$  where  $b_j^i$  is either 0 or 1 in a way that  $z^i = (1/2) \times (1 + \sum_{j=1}^{52} b_j^i 2^{-j})$ . Then the point  $(z^1, \dots, z^N)$  in  $N$ -dimension can be expressed by  $52 \times N$  binary numbers. Interleaving the binary coordinate values yields binary values. Connecting the binary values in their numerical order produces the Morton ordering. Then an appropriate coarse-graining leads to the subdivision of a box. For examples, when  $N = 2$ , the binary value corresponding  $(z^1, z^2)$  is  $b_1^1 b_1^2 b_2^1 b_2^2 \dots b_{52}^1 b_{52}^2$ . The point is in first quadrant if  $(b_1^1, b_1^2) = (1, 1)$ , in second quadrant if  $(b_1^1, b_1^2) = (0, 1)$ , in third quadrant if  $(b_1^1, b_1^2) = (0, 0)$  and in fourth quadrant if  $(b_1^1, b_1^2) = (1, 0)$ . Applying this classification to a number of particles produces  $2^2$  disjoint subsets of clustered particles. Similarly, using  $b_1^1 b_1^2 b_2^1 b_2^2$  and ignoring the rest subgrid scales gives  $4^2$  subsets when  $N = 2$ . Using affine transformation when the particles are not in  $[0.5, 1)^N$ , the Morton ordering within floating-point context provides an efficient way to patch the particles.

Note that the inequality  
(5.14)

$$\left| \left( \Phi_{\mathcal{D},(u,r)}^{m,j}(\mu^0) - \widehat{\Phi}_{\mathcal{D},(u,r)}^{m,j}(\mu^0), P_{T-t_j} f \right) \right| \leq \frac{C u_j^{r_j+1}}{(r_j + 1)!} \| P_{T-t_j} f \|_{\text{Lip}(r_j+1)}$$

holds from Eq. (4.6) when  $f$  is a Lipschitz function. One can use Eq. (5.14) and Eq. (5.12) to quantify the patch size  $u_j$  satisfying Eq. (5.13) for a fixed  $r_j$  in terms of the Lipschitz norm of  $f$ .

**6. Numerical simulations.** We here perform numerical simulations to examine the efficiency and accuracy of the proposed filtering approaches. We introduce the test model in subsection 6.1 and apply the Kalman filter



to obtain its exact solution in subsection 6.2. Subsequently we obtain particle approximations from a Monte-Carlo sampling in subsection 6.3 and from PPF and APPF with cubature on Wiener space of degree  $m = 5$  in subsection 6.4. Finally, in subsection 6.5, we study the prospective performance of PPF and APPF with cubature on Wiener space of degree  $m = 7$ .

6.1. *Test model.* Consider the stochastic differential equation

$$(6.1) \quad dX = d \begin{pmatrix} x^1 \\ x^2 \\ x^3 \end{pmatrix} = \left[ -\Lambda X + a_0 \begin{pmatrix} 0 \\ -x^1 x^3 \\ x^1 x^2 \end{pmatrix} \right] dt + g I_3 dW$$

in three dimension where  $\Lambda = \begin{pmatrix} \sigma & -\sigma & 0 \\ -\rho & 1 & 0 \\ 0 & 0 & \beta \end{pmatrix}$ ,  $dW = (dW_1 \ dW_2 \ dW_3)^t$

and  $I_3$  denotes the  $3 \times 3$  identity matrix. Here the superscript  $t$  denotes the transpose. When  $a_0 = 1$ , Eq. (6.1) is the Lorenz-63 model that has been intensively studied in the data assimilation community [25, 27, 39]. When  $a_0 = 0$ , Eq. (6.1) is the Ornstein-Uhlenbeck process [35] and this linear process is our test model. The parameter values  $\sigma = 1$ ,  $\rho = 0.28$ ,  $\beta = 8/3$  and  $g = 0.5$  are used.

For the observation process, we take the identity function for  $\varphi(\cdot)$  in Eq. (4.2), and

$$(6.2) \quad Y_n = X_n + \eta_n, \quad \eta_n \sim \mathcal{N}(0, R_n).$$

The inter-observation time is  $T = 0.5$  and the cases are studied in which the covariance of observation noise is  $R_n = R \times I_3$  for a number of values  $R = 10^{-1}, 10^{-2}$  and  $10^{-3}$ .

6.2. *Kalman filter.* For Eq. (6.1) where  $a_0 = 0$  and Eq. (6.2), the conditioned measure is Gaussian and  $\pi_{n|n'} = \mathcal{N}(M_{n|n'}, C_{n|n'})$  can be obtained using the Kalman filter. In this case, the prior covariance  $C_{n|n-1}$  satisfies the Riccati difference equation and its solution converges as  $n$  increases (see [3] for the conditions). We take the measure  $\pi_{0|0}$  so that  $C_{n|n-1}$  and  $C_{n|n}$  do not depend on  $n$ . We see that the diagonal element of  $C_{n|n-1}$  are about  $10^{-1}$  for all cases of  $R = 10^{-1}, 10^{-2}, 10^{-3}$ . The diagonal element of  $C_{n|n}$  are about  $10^{-1}$  when  $R = 10^{-1}$ , about  $10^{-2}$  when  $R = 10^{-2}$  and about  $10^{-3}$  when  $R = 10^{-3}$ .

We apply the Kalman filter for  $1 \leq n \leq 10^8$  and calculate the values of  $D_1, D_2$  and  $D_3$  satisfying  $y_n = M_{n|n-1} + (D_1 \ D_2 \ D_3)^t \cdot \sqrt{\text{diag}(C_{n|n-1})}$ .

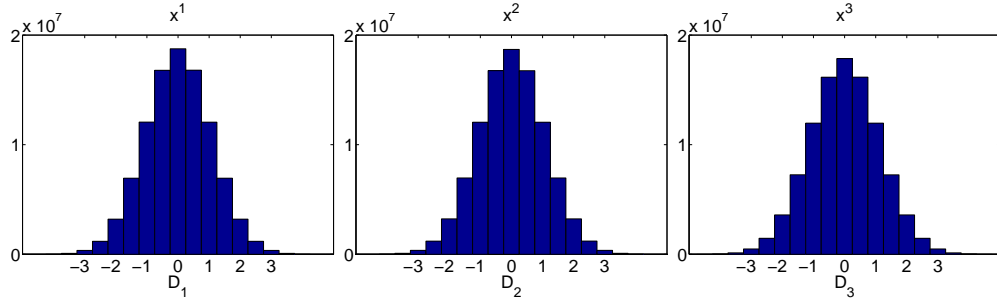


FIG 1. The distribution of normalized distances between the observation and the prior mean when the noise covariance is  $R_n = 10^{-2} \times I_3$ .

The histograms in Fig. 1 show the distribution of these normalized distances between the observation and the prior mean when  $R = 10^{-2}$  (the cases of  $R = 10^{-1}$  and  $R = 10^{-3}$  are similar and not shown). One can see that most of the observations are within two times the standard deviations from the prior mean in each coordinate. Among the cases of  $10^8$ , there are 4,592,208 cases for which  $|D_i| > 1$  for all  $i = 1, 2, 3$  at the same time. There are 37,574 cases for which  $|D_i| > 2$  for all  $i$  at the same time, and 60 cases for which  $|D_i| > 3$  for all  $i$  at the same time. In the following, we study the cases when the parameter value of  $D \equiv D_1 = D_2 = D_3$  is 1, 2 and 3. These three cases correspond to normal, exceptional and rare event, respectively.

6.3. *Monte-Carlo samples.* In order to quantify the accuracy of the discrete measures given in the form of Eq. (3.1), we define the  $L^2$  norm of the moment as the following. Let  $\mathcal{C}^p$  be the  $p$ -th moment of  $X = (x^1 \ x^2 \ x^3)^t$ , i.e.,

$$\mathcal{C}_{i_1, \dots, i_p}^p = \mathbb{E} \left( \prod_{j=1}^p (x^{i_j} - \mathbb{E}(x^{i_j})) \right)$$

where  $i_j = 1, 2, 3$ . The  $L^2$  norm of  $\mathcal{C}^p$  is defined by

$$(6.3) \quad \|\mathcal{C}^p\|_2 \equiv \left( \sum_{i_1, \dots, i_p=1}^3 |\mathcal{C}_{i_1, \dots, i_p}^p|^2 \right)^{1/2}.$$

When  $p = 1$ , Eq. (6.3) is the Euclidean norm of the vector. It is the Frobenius norm of the matrix when  $p = 2$ . The relative root mean square error

$$(6.4) \quad \text{rmse}\% \equiv \|\mathcal{C}^p - \widehat{\mathcal{C}}^p\|_2 / \|\mathcal{C}^p\|_2$$

TABLE 1  
The number of adaptive partition  $k$  for KLV with  $m = 5$

	$\epsilon = 10^{-2}$	$\epsilon = 10^{-3}$	$\epsilon = 10^{-4}$	$\epsilon = 10^{-5}$
$R = 10^{-1}$	7	31	102	344
$R = 10^{-2}$	10	29	101	330
$R = 10^{-3}$	20	48	120	329

is used to measure the accuracy of the moment approximations, where  $\widehat{\mathcal{C}}^p$  is the  $p$ -th moment of a particle approximation.

We perform a Gaussian sampling from the prior and the posterior (the samples are not obtained from the integration of Eq. (6.1) but drawn from the analytic solution). We also apply bootstrap reweighting to the prior samples so that it approximates the posterior. The values of Eq. (6.4) are depicted in Figs. 3(a), 3(c), 3(e), 3(g) when  $R = 10^{-2}$ ,  $D = 1, 2, 3$  and in Figs. 4(a), 4(b), 4(d), 4(e), 4(g), 4(h) when  $D = 1$ ,  $R = 10^{-1}, 10^{-2}, 10^{-3}$ . As the number of samples  $M$  increases, the error of Eq. (6.4) asymptotically behaves  $M^{-1/2}$  in all cases. The results will be used as the benchmark calculations for the accuracy of PPF and APPF.

6.4. *PPF and APPF with cubature on Wiener space of degree 5.* We here apply PPF and APPF at the flow level. In case of  $d = 3$ , i.e., the system is driven by three independent white noises, cubature on Wiener space of degree  $m = 3$  and  $m = 5$ , with support size  $n_m = 6$  and  $n_m = 28$  respectively, are available. We use the KLV operator with degree  $m = 5$ .

We use the adaptive partition for both PPF and APPF. In order to do that, the partition  $\mathcal{D}(\epsilon, g^{y_n})$  satisfying Eq. (5.10) with  $\widetilde{Q}_{s_j}^m$  in place of  $Q_{s_j}^m$  is analytically obtained for the system of Eq. (6.1) where  $a_0 = 0$ . Note that the likelihood  $g^{y_n}$  is the density function of  $\mathcal{N}(y_n, R_n)$  and that the adaptive partition does not depend on  $y_n$  but on  $R_n$  or Lipschitz norm of  $g^{y_n}$ . The number of iterations  $k$  as a function of  $\epsilon$  and  $R$  is listed in table 1.

For the recombination of the PPF, we use a variant of the adaptive recombination. It requires to satisfy Eq. (5.13) with  $f = g^{y_n}$  for all  $y_n \in \mathbb{R}^N$ , i.e.,

$$(6.5) \quad \sup_{y_n} \left| \left( \Phi_{\mathcal{D},(u,r)}^{m,j}(\mu^0) - \widehat{\Phi}_{\mathcal{D},(u,r)}^{m,j}(\mu^0), P_{T-t_j} g^{y_n} \right) \right| < \theta$$

so that the recombination does not depend on  $y_n$  but on  $R_n$ . We choose the recombination degree  $r = 5$  and simulate the PPF for the cases of  $\epsilon = 10^{-2}, 10^{-3}$  with  $\theta = 0.3 \times \epsilon$ .

For the APPF, the tolerance  $\tau$  has to be specified in addition to the parameters  $\{\epsilon, \theta\}$ . The value of  $\tau$  varies in each case, but we choose it so

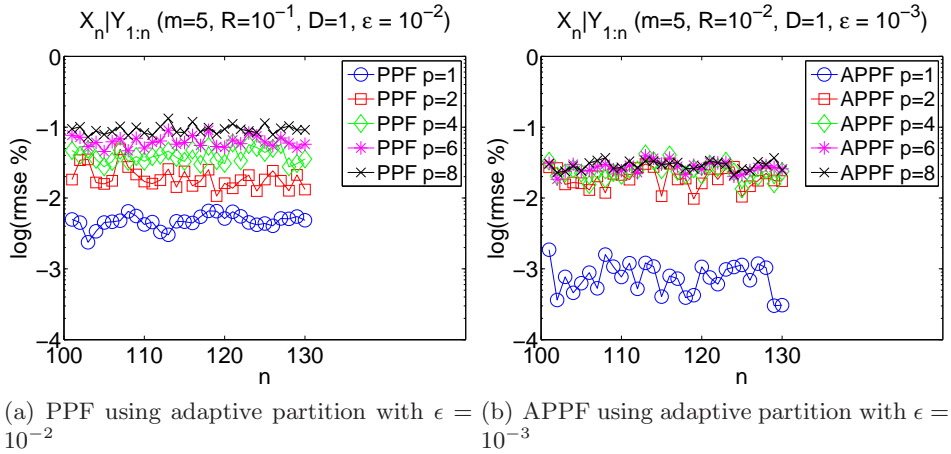


FIG 2. The relative  $L^2$  errors for the  $p$ -th moments of the evolutionary posterior.

that the ADA operator in Eq. (4.33) allows  $1/4 \sim 1/3$  part of particles leap to the next observation time for all iterations except the first and last few steps. The remaining particles are reduced by the adaptive recombination, i.e., the recombination satisfies

$$(6.6) \quad \left| \left( \Phi_{\mathcal{D},(u,r),\tau}^{m,j}(\mu^0) - \widehat{\Phi}_{\mathcal{D},(u,r),\tau}^{m,j}(\mu^0), P_{T-t_j} g^{y_n} \right) \right| < \theta$$

where  $\mu^0 = \tilde{\pi}_{n-1|n-1}^{\text{APPF}}$ . We again choose the recombination degree  $r = 5$  and simulate the APPF for the cases of  $\epsilon = 10^{-2}, 10^{-3}$  with  $\theta = 0.3 \times \epsilon$ .

With the value of  $D$  being fixed, we apply PPF and APPF to obtain the values of Eq. (6.4) for the evolutionary posterior. Fig. 2 shows that two filtering algorithms are stable and that our numerical error estimates can be trusted (the rest cases produce similar plots and are not shown).

In our numerical simulations, the number of patches needed to satisfy Eq. (6.5) in the PPF increases as the time partition approaches the next observation time, finally about  $8^3 \sim 16^3$ . On the contrary, Eq. (6.6) in the APPF is satisfied with  $2^3 (< 10)$  patches in most cases. As a result, APPF saves computation time significantly compared with PPF.

When  $R = 10^{-2}$  is fixed and  $D = 1, 2, 3$  varies, the relative  $L^2$  errors of the  $p$ -th moments of PPF and APPF are shown in Figs. 3(b), 3(d), 3(f), 3(h). We examine two cases of  $\epsilon = 10^{-2}$  and  $\epsilon = 10^{-3}$ . The recombination times are measured using Visual Studio with Intel 2.53 GHz processor (the autonomous ODEs are solved analytically). Fig. 3 reveals the following.

- The prior approximation of PPF with  $\epsilon = 10^{-3}$  shows similar accuracy

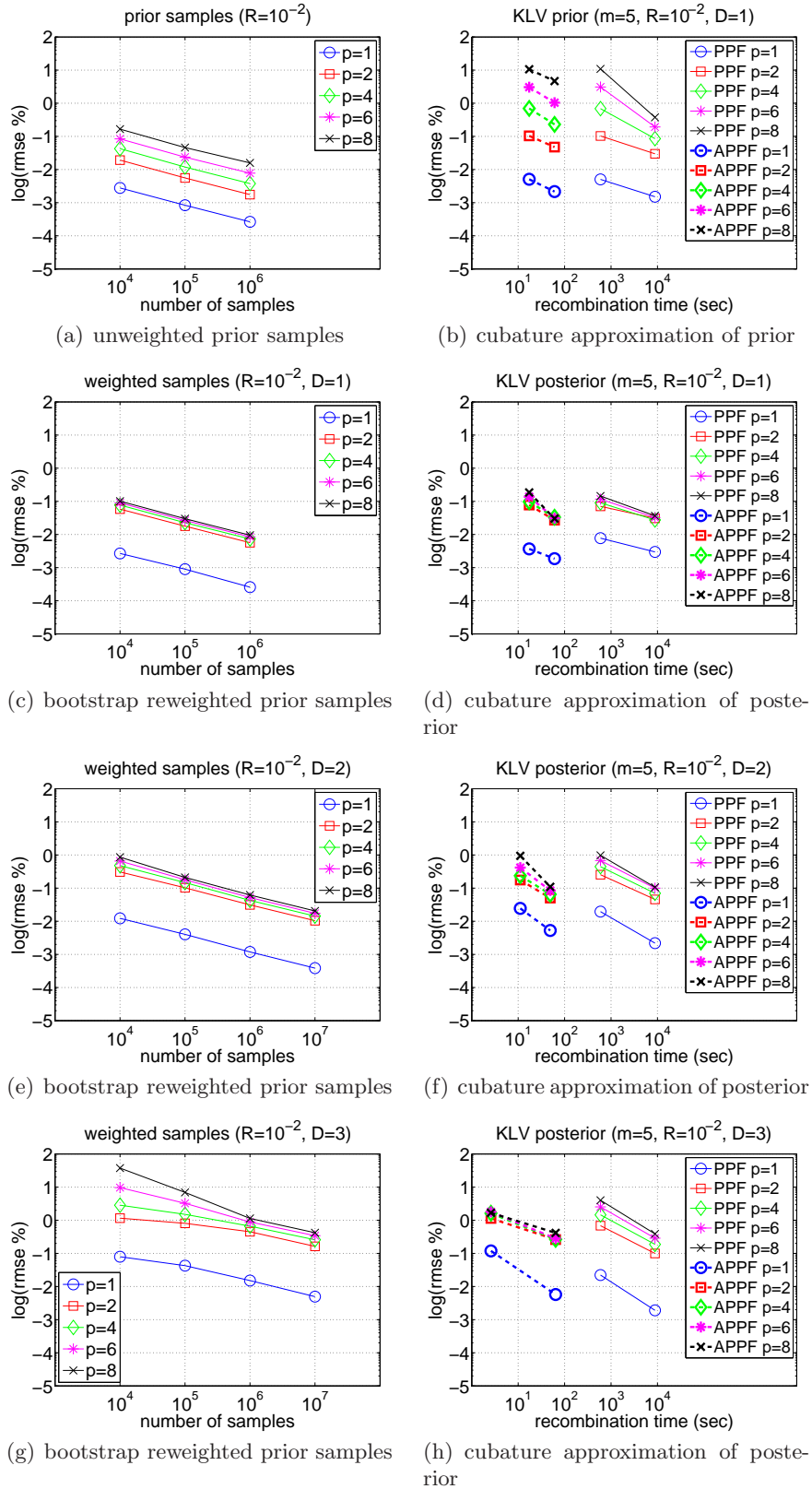


FIG 3. The prior and posterior approximations when  $R = 10^{-2}$  is fixed and  $D = 1, 2, 3$  varies. The left column is from Monte-Carlo samples and the right column is from cubature approximation when  $\epsilon = 10^{-2}, 10^{-3}$ . The top first row is for the prior and the bottom three rows are for the posterior.

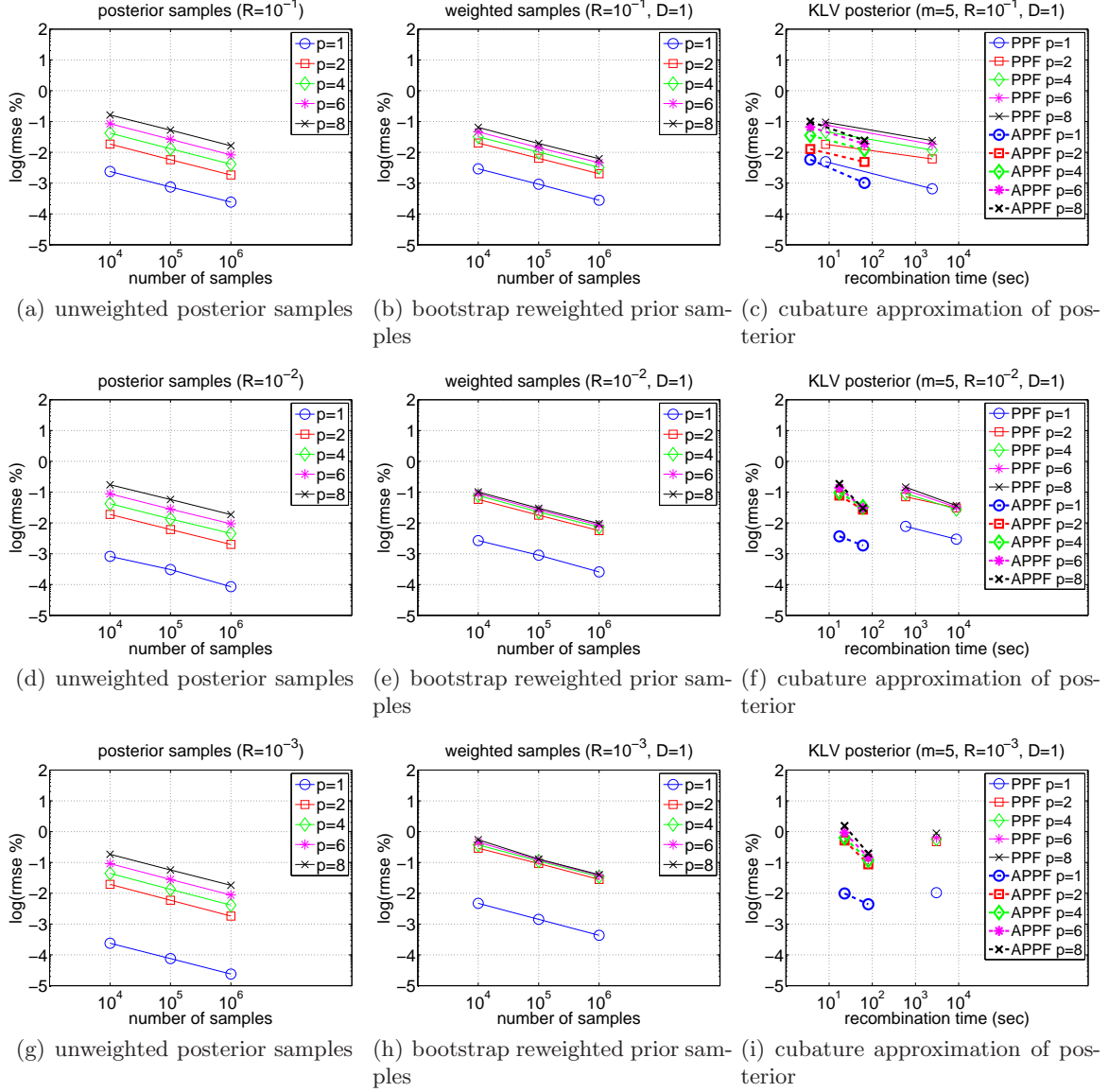


FIG 4. The posterior approximations when  $D = 1$  is fixed and  $R = 10^{-1}, 10^{-2}, 10^{-3}$  varies. The left and middle columns are from Monte-Carlo samples and the right column is from cubature approximation when  $\epsilon = 10^{-2}, 10^{-3}$ . In Fig. 4(i), the PPF with  $\epsilon = 10^{-3}$  is not produced.

with  $10^4$  Monte-Carlo sampling (Figs. 3(a), 3(b)).

- The accuracy of the APPF prior approximation is in general worse than PPF especially for higher order moments (Fig. 3(b)).
- As the observation is located far from the prior mean, i.e., as  $D$  increases, the posterior approximation obtained from Monte-Carlo bootstrap reweighting becomes less accurate (Figs. 3(c), 3(e), 3(g)).
- The accuracy of the APPF posterior approximation is similar to PPF but APPF significantly reduces the recombination time (Figs. 3(d), 3(f), 3(h)).
- The accuracy of the PPF and APPF posterior approximations with  $\epsilon = 10^{-2}$  is similar to  $10^4$  Monte-Carlo reweighted samples when  $D = 1, 2$  (Figs. 3(c), 3(d), 3(e), 3(f)) and to  $10^5$  reweighted samples when  $D = 3$  (Figs. 3(g), 3(h)).
- The accuracy of the PPF and APPF posterior approximations with  $\epsilon = 10^{-3}$  is similar to  $10^5$  Monte-Carlo reweighted samples when  $D = 1$  (Figs. 3(c), 3(d)), to  $10^6$  reweighted samples when  $D = 2$  (Figs. 3(e), 3(f)) and to  $10^7$  reweighted samples when  $D = 3$  (Figs. 3(g), 3(h)).

There is an important insight to be gained from this experimental analysis. Though PPF produces a better description of the prior than APPF, this naive approximation of the prior is not good at describing the fundamental object of interest in filtering, i.e., the posterior. The point is that one needs an extremely accurate representation of the prior in certain localities. The APPF delivers this without undue cost. The PPF method would have to deliver this accuracy uniformly and well out into the tail of the prior. As a result, PPF and APPF succeed in accurately describing the higher order statistics of posterior even when  $D$  is big and Monte-Carlo fails to do such a job.

When  $D = 1$  is fixed and  $R = 10^{-1}, 10^{-2}, 10^{-3}$  varies, the values of Eq. (6.4) for PPF and APPF are shown in Figs. 4(c), 4(f), 4(i). We again examine two cases of  $\epsilon = 10^{-2}$  and  $\epsilon = 10^{-3}$ . Fig. 4 reveals the following.

- The moment approximations of Monte-Carlo Gaussian samples are insensitive to the covariance (recall that the diagonal element of  $C_{n|n}$  is almost the same with the value of  $R$ ) except the mean (Figs. 4(a), 4(d), 4(g)).
- As the observation is more accurate, i.e., as  $R$  decreases, the posterior approximation obtained from Monte-Carlo bootstrap reweighting becomes less accurate (Figs. 4(b), 4(e), 4(h)).
- As  $R$  decreases, the recombination time needed to achieve a given degree of accuracy becomes bigger for PPF but this is not the case

TABLE 2  
*The number of adaptive partition  $k$  for FGC with  $m = 7$*

	$\epsilon = 10^{-2}$	$\epsilon = 10^{-3}$	$\epsilon = 10^{-4}$	$\epsilon = 10^{-5}$
$R = 10^{-1}$	2	4	6	10
$R = 10^{-2}$	5	9	16	28
$R = 10^{-3}$	9	17	30	54

for APPF, i.e., the recombination time for APPF is insensitive to  $R$  (Figs. 4(c), 4(f), 4(i)).

The simulations show that the APPF becomes more competitive than the PPF for the solution of the intermittent data assimilation problem with small observation noise error. It further shows that the APPF is of higher order with respect to the recombination time and can achieve the given degree of accuracy with lower computational cost.

Although  $Y_n$  is “there and measurable” it is sometimes the case that it is actually computationally very expensive to compute and that actually the thing one can compute is the evaluation of likelihood for a number of locations. For example, consider a tracking problem for an object of moderate intensity and diameter that does a random walk and is moving against a slightly noisy background and is observed relatively infrequently. Its influence is entirely local. The likelihood function will be something like the Gaussian centred at the position of object but completely uninformative elsewhere in the space. The smaller the object, the tighter or narrower the Gaussian the harder the problem of finding the object becomes. One can compute the likelihood at any point in the space, but only evaluations at the location of the particle are informative. In that way one sees that

1. The  $Y_n$  is “observable” but only partially observed - and with low noise is very expensive to observe accurately as one has to find the particle.
2. The likelihood can be observed at points in the space.

In this sort of example it would be quite wrong to assume that, if we know the prior distribution of  $X_n$  then just because  $Y_n = X_n + \eta_n$  we know the posterior distribution at zero cost. For sequential Monte-Carlo methods, bootstrap reweighting would seem to give a much better approach.

6.5. *Prospective performance PPF and APPF with cubature on Wiener space of degree 7.* A cubature formula on Wiener space of degree  $m = 7$  is currently not available when  $d = 3$ . Here we use another operator to see the prospective performance of higher order cubature formula.



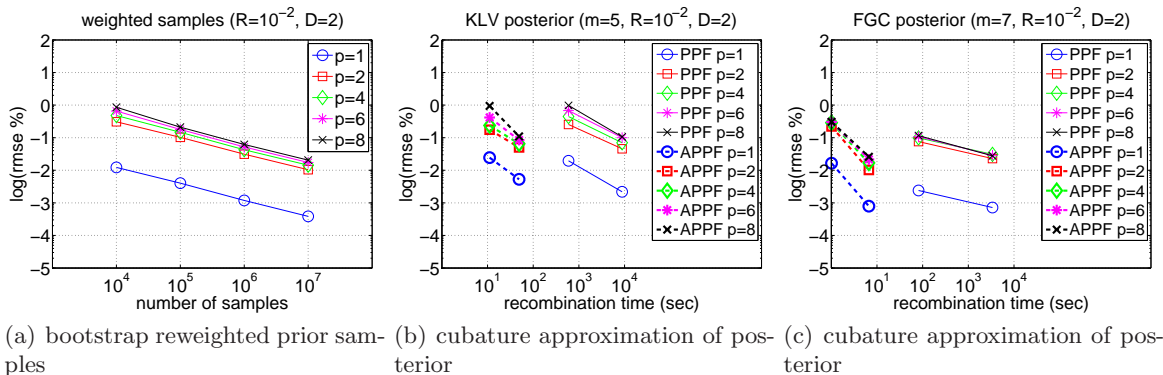


FIG 5. The posterior approximations when  $R = 10^{-2}$  and  $D = 2$ . The left is from Monte-Carlo samples and the middle and right is from cubature approximation when  $\epsilon = 10^{-2}, 10^{-3}$ .

For the linear dynamics satisfying

$$X(\Delta) = F_{\Delta}X(0) + \nu_{\Delta}, \quad \nu_{\Delta} \sim \mathcal{N}(0, Q_{\Delta})$$

for which  $F_{\Delta} \in \mathbb{R}^{3 \times 3}$  is a matrix, one can define the forward operator

$$(6.7) \quad \text{FGC}^{(m)} \left( \sum_{i=1}^n \kappa_i \delta_{x^i}, \Delta \right) \equiv \sum_{i=1}^n \sum_{j=1}^{n_m} \kappa_i \lambda_j \delta_{F_{\Delta} x^i + z^j}$$

where  $\{\lambda_j, z^j\}_{j=1}^{n_m}$  is a Gaussian cubature of degree  $m$  with respect to the law of  $\nu_{\Delta}$ . The authors see that the performance of FGC is similar to KLV on the flow level when  $m = 3, 5$  and that Eq. (6.7) can be used as an alternative to Eq. (5.7) for the PPF and APPF application to the test model, i.e., Eq. (6.1) where  $a_0 = 0$ .

The number of iterations  $k$  in the adaptive partition, obtained from using FGC with Gauss-Hermite cubature of degree  $m = 7$  whose support size is  $n_m = 64$  in place of  $Q_{s_j}^m$ , is shown in table 2. We apply FGC with degree  $m = 7$  to obtain a prior and posterior approximation, where the recombination degree  $r = 5$  and  $\theta = 0.2 \times \epsilon$  is used. Our choice of  $\tau$  is again such that  $1/4 \sim 1/3$  of the particles are allowed to skip to the next observation time. Eq. (6.4) in the case of  $R = 10^{-2}$ ,  $D = 2$  and  $\epsilon = 10^{-2}, 10^{-3}$  is shown in Fig. 5(c), that can be viewed as an accuracy of PPF and APPF with cubature on Wiener space of degree  $m = 7$ . Its performance is in fact one higher order improvement for both accuracy and recombination time in view of Figs. 5(a), 5(b). This result highlights the necessity to find cubature formula on Wiener

space of degree  $m = 7$  in order to solve the PDE or filtering problem with high accuracy in a moderate dimension.

**7. Discussion.** In this paper we introduce a hybrid methodology for the numerical resolution of the filtering problem which we call the adaptive patched particle filter (APPF). We explore some of its properties and we report on a first attempt at a practical implementation. The APPF combines many different “methods”, each of which addresses a different part of the problem and has independent interest. At a fundamental level all of the methods use high order approaches to quantify uncertainty (cubature), and also to reduce the complexity of calculations (recombination based on heavy numerical linear algebra), while retaining explicit thresholds for accuracy in the individual computation. The thresholds for accuracy in a stage are normally achievable in a number of ways (e.g., small time step with low order, or large time step with high order) and the determination of these choices depends on computational cost. Aside from this use of the error threshold and choices based on computational efficiency there are several other points to observe in our development of this filter.

1. One feature is the surprising ease with which one can adapt the computations to the observational data and so avoid performing unnecessary computations. In even moderate dimensions (we work in  $3 + 1$ ) this has a huge impact for the computation time while preserving the accuracy we achieve for the posterior distribution (Figs. 3(d), 3(f), 3(h), Figs. 4(c), 4(f), 4(i)). It is an automated form of high order importance sampling which has wider application than the one explored in this paper, for instance it is used to deliver accurate answers to PDE problems with piecewise smooth test function in the example developed in [23].
2. Another innovation allowing a huge reduction in computation is the ability to efficiently “patch the particles” in the multiple dimensional scenario. Although the problem might at first glance seem elementary, it is in fact the problem of data classification. To resolve this problem we introduce an efficient algorithm for data classification based on extending the Morton order to floating point context. This method has now also been used effectively for efficient function extrapolation [30].
3. The KLV algorithm is at the heart of a number of successful methods for solving PDEs in moderate dimension [29]. In each case, something has to be done about the explosion of scenarios after each time step; this in turn has to rely on and understanding the errors. In this paper

we take a somewhat different approach to the literature [26] in the way we use higher order Lipschitz norms systematically to understand how well functions have been smoothed, and to measure the scales on which they can be well approximated by polynomials. This has the consequence that one can be quite precise about the errors one incurs at each stage in the calculation. In the end this is actually quite crucial to the logic of our approach since an efficient method requires optimisation over several parameters - something that is only meaningful if there are (at least in principle) uniform estimates on errors. As a result of this perspective, we do not follow the time steps and analytic estimates introduced by Kusuoka in [21] although we remain deeply influenced by balancing the smoothing properties of the semigroup with the use of non-equidistant time steps.

4. The focus on Lipschitz norms makes it natural to apply an adaptive approach to the recombination patches as well as to the prediction process. In both cases we can be lead by the local smoothness of the likelihood function as sampled on our high order high accuracy set of scenarios.
5. We have focussed our attention on the quality of the tail distribution of the approximate posterior we construct. This is important in the filtering problem because a failure to describe the tail behaviour of the tracked object implies that one will lose the trajectory all together at some point. These issues are particularly relevant in high dimensions as the cost of increasing the frequency of observation can be prohibitive. If one wishes to ensure reliability of the filter in the setting where there is a significant discrepancy between the prior estimate and the realised outcome over a time step then our APPF with cubature on Wiener space of degree 5 already shows in the three dimensional example that it can completely outperform sequential importance resampling Monte-Carlo approach. The absence, at the current time, of higher order cubature formulae is in this sense very frustrating as the evidence we give suggests that higher degree methods will lead to substantial further benefits for both computation and accuracy.

In putting this paper together we have realised that there are many branches in this algorithm that can be improved, in particular some parts of the adaptive process and also the recombination (a theoretical improvement in the order of recombination has recently been discovered [34]). There are also large parts that can clearly be parallelised. We believe that there is ongoing scope for increasing the performance of the APPF.

**Acknowledgment.** The authors would like to thank the following institutions for their financial support of this research. Wonjung Lee : NCEO project NERC and King Abdullah University of Science and Technology (KAUST) Award No. KUK-C1-013-04. Terry Lyons : NCEO project NERC, ERC grant number 291244 and EPSRC grant number EP/H000100/1. The authors also thank the Oxford-Man Institute of Quantitative Finance for its support.

## References.

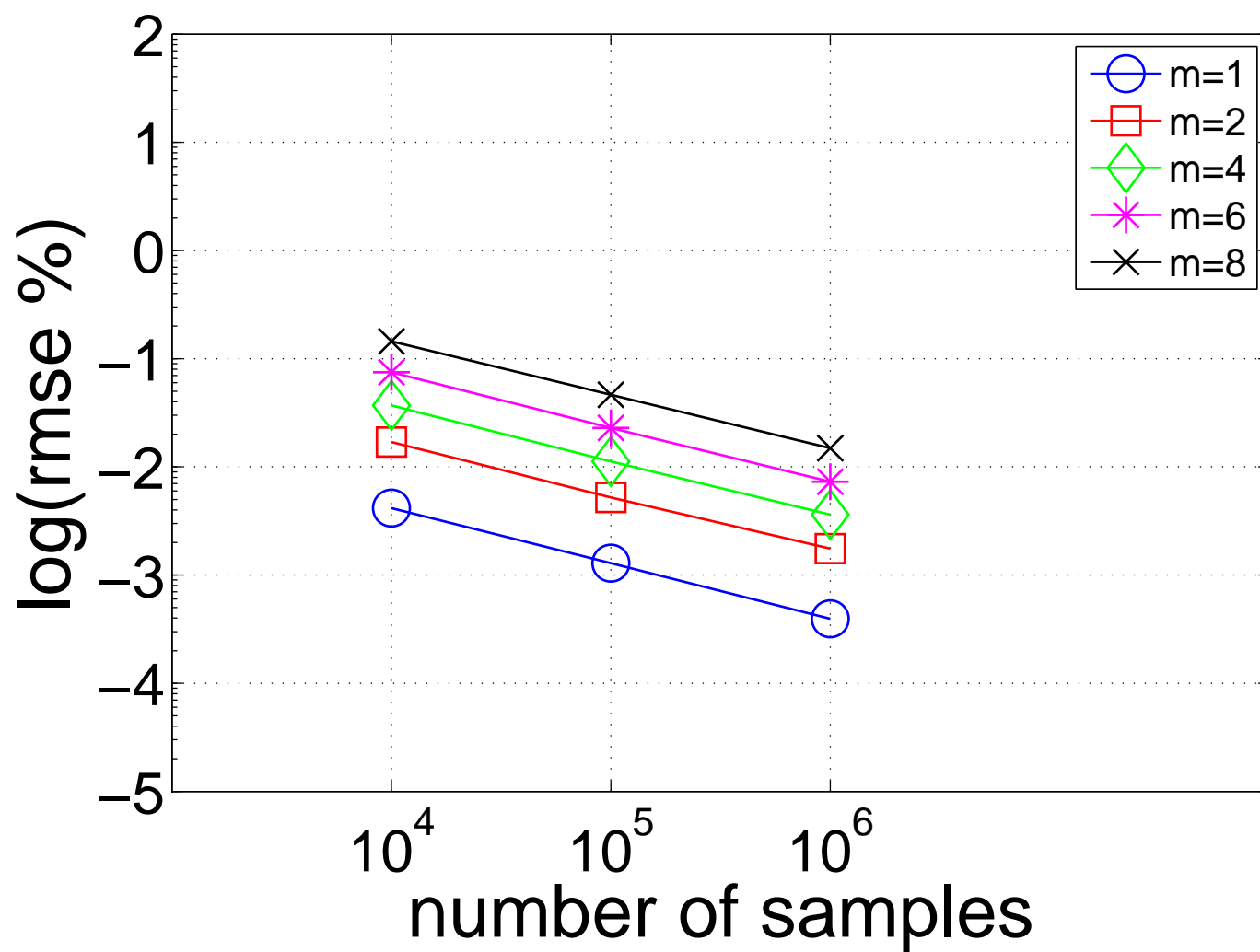
- [1] ANDERSON, B. D. O. and MOORE, J. B. (1979). *Optimal filtering* **11**. Prentice-hall Englewood Cliffs, NJ.
- [2] BENEŠ, V. (1981). Exact finite-dimensional filters for certain diffusions with nonlinear drift. *Stochastics: An International Journal of Probability and Stochastic Processes* **5** 65–92.
- [3] BITMEAD, R. R. and GEVERS, M. (1991). Riccati difference and differential equations: Convergence, monotonicity and stability. *The Riccati Equation* 263–291.
- [4] CARPENTER, J., CLIFFORD, P. and FEARNHEAD, P. (1999). Improved particle filter for nonlinear problems. In *Radar, Sonar and Navigation, IEE Proceedings-* **146** 2–7. IET.
- [5] CRISAN, D. and DOUCET, A. (2002). A survey of convergence results on particle filtering methods for practitioners. *Signal Processing, IEEE Transactions on* **50** 736–746.
- [6] CRISAN, D. and GHAZALI, S. (2006). On the convergence rates of a general class of weak approximations of SDEs. *Stochastic differential equations: theory and applications* **2** 221–248.
- [7] CRISAN, D. and LYONS, T. (2002). Minimal entropy approximations and optimal algorithms for the filtering problem. *Monte Carlo methods and applications* **8** 343–356.
- [8] DOUCET, A., DE FREITAS, N. and GORDON, N. (2001). *Sequential Monte Carlo methods in practice*. Springer Verlag.
- [9] DOUCET, A., GODSILL, S. and ANDRIEU, C. (2000). On sequential Monte Carlo sampling methods for Bayesian filtering. *Statistics and computing* **10** 197–208.
- [10] EVENSEN, G. (2009). *Data assimilation: the ensemble Kalman filter*. Springer Verlag.
- [11] GELB, A. (1974). *Applied optimal estimation*. MIT press.
- [12] GORDON, N. J., SALMOND, D. J. and SMITH, A. F. M. (1993). Novel approach to nonlinear/non-Gaussian Bayesian state estimation. In *Radar and Signal Processing, IEE Proceedings F* **140** 107–113. IET.
- [13] GYURKÓ, L. G. and LYONS, T. J. (2011). Efficient and practical implementations of Cubature on Wiener space. *Stochastic Analysis 2010* 73–111.
- [14] JAZWINSKI, A. (1970). *Stochastic Processes and Filtering Theory*, Vol. 64. San Diego, California: Mathematics in Science and Engineering.
- [15] KALMAN, R. E. and BUCY, R. S. (1961). New results in linear filtering and prediction theory. *Journal of Basic Engineering* **83** 95–108.
- [16] KALMAN, R. E. et al. (1960). A new approach to linear filtering and prediction problems. *Journal of basic Engineering* **82** 35–45.
- [17] KLOEDEN, P. E. and PLATEN, E. (2011). *Numerical solution of stochastic differential equations* **23**. Springer.

- [18] KUSHNER, H. (1967). Approximations to optimal nonlinear filters. *Automatic Control, IEEE Transactions on* **12** 546–556.
- [19] KUSUOKA, S. (2001). Approximation of expectation of diffusion process and mathematical finance. *Advanced Studies in Pure Mathematics* **31** 147–165.
- [20] KUSUOKA, S. (2003). Malliavin calculus revisited. *J. Math. Sci. Univ. Tokyo* **10** 261–277.
- [21] KUSUOKA, S. (2004). Approximation of expectation of diffusion processes based on Lie algebra and Malliavin calculus. In *Advances in mathematical economics* 69–83. Springer.
- [22] KUSUOKA, S. and STROOCK, D. (1987). Applications of the Malliavin calculus. III.
- [23] LITTERER, C. and LYONS, T. (2012). High order recombination and an application to cubature on Wiener space. *The Annals of Applied Probability* **22** 1301–1327.
- [24] LIU, J. S. and CHEN, R. (1998). Sequential Monte Carlo methods for dynamic systems. *Journal of the American statistical association* **93** 1032–1044.
- [25] LORENZ, E. N. (1963). Deterministic nonperiodic flow. *Journal of the atmospheric sciences* **20** 130–141.
- [26] LYONS, T. and VICTOIR, N. (2004). Cubature on Wiener space. *Proceedings of the Royal Society of London. Series A: Mathematical, Physical and Engineering Sciences* **460** 169–198.
- [27] MILLER, R. N., CARTER JR, E. F. and BLUE, S. T. (1999). Data assimilation into nonlinear stochastic models. *Tellus A* **51** 167–194.
- [28] MORTON, G. M. (1966). *A computer oriented geodetic data base and a new technique in file sequencing*. International Business Machines Company.
- [29] NINOMIYA, S. and VICTOIR, N. (2008). Weak approximation of stochastic differential equations and application to derivative pricing. *Applied Mathematical Finance* **15** 107–121.
- [30] PAN, W. Cubature and TARN option pricing. unpublished.
- [31] PITT, M. K. and SHEPHARD, N. (1999). Filtering via simulation: Auxiliary particle filters. *Journal of the American statistical association* **94** 590–599.
- [32] PUTINAR, M. (1997). A note on Tchakaloff’s theorem. *Proceedings of the American Mathematical Society* **125** 2409–2414.
- [33] STEIN, E. M. (1993). *Singular Integrals and Differentiability Properties of Functions*. 1970. Princeton, New Jersey.
- [34] TCHERNYCHOVA, M. private communication.
- [35] UHLENBECK, G. E. and ORNSTEIN, L. S. (1930). On the theory of the Brownian motion. *Physical Review* **36** 823.
- [36] VAN LEEUWEN, P. J. (2010). Nonlinear data assimilation in geosciences: an extremely efficient particle filter. *Quarterly Journal of the Royal Meteorological Society* **136** 1991–1999.
- [37] WATANABE, N. I. S. and IKEDA, N. (1981). *Stochastic differential equations and diffusion processes*. North Holland Math. Library/Kodansha, Amsterdam/Tokyo.
- [38] WENDLAND, H. (2005). *Scattered data approximation* **2**. Cambridge University Press Cambridge.
- [39] XIONG, X., NAVON, I. M. and UZUNOGLU, B. (2006). A note on the particle filter with posterior Gaussian resampling. *Tellus A* **58** 456–460.

WONJUNG LEE  
STOCHASTIC ANALYSIS GROUP AND OCCAM  
MATHEMATICAL INSTITUTE  
AND  
OXFORD-MAN INSTITUTE OF QUANTITATIVE FINANCE  
UNIVERSITY OF OXFORD  
U.K.  
E-MAIL: [leew@maths.ox.ac.uk](mailto:leew@maths.ox.ac.uk)

TERRY LYONS  
STOCHASTIC ANALYSIS GROUP  
MATHEMATICAL INSTITUTE  
AND  
OXFORD-MAN INSTITUTE OF QUANTITATIVE FINANCE  
UNIVERSITY OF OXFORD  
U.K.  
E-MAIL: [tlyons@maths.ox.ac.uk](mailto:tlyons@maths.ox.ac.uk)

$r=10^{-1}$



FGC posterior,  $R=10^{-2}$ ,  $D=2$

